Advanced Review

Spin-restricted ensemble-referenced Kohn–Sham method: basic principles and application to strongly correlated ground and excited states of molecules

Michael Filatov*

Ensemble density functional theory (DFT) is a novel theoretical approach that is capable of exact treatment of non-dynamic electron correlation in the ground and excited states of many-body fermionic systems. In contrast to ordinary DFT, ensemble DFT has not found so far a way to the repertoire of methods of modern computational chemistry, probably owing to the lack of practically affordable implementations of the theory. The spin-restricted ensemble-referenced Kohn–Sham (REKS) method represents perhaps the first computational scheme that makes ensemble DFT calculations feasible. The REKS method is based on the rigorous ensemble representation of the energy and the density of a strongly correlated system and provides for an accurate and consistent description of molecular systems the electronic structure of which is dominated by the non-dynamic correlation. This includes the ground and excited states of molecules undergoing bond breaking/bond formation, the low-spin states of biradicals and polyradicals, symmetry forbidden chemical reactions and avoided crossings of potential energy surfaces, real intersections between the energy surfaces of the ground and excited states (conical intersections), and many more. The REKS method can be employed in connection with any local, semi-local and hybrid (global and range-separated) functional and affords calculations of large and very large molecular systems at a moderate mean-field cost.

How to cite this article:
WIREs Comput Mol Sci 2015. doi: 10.1002/wcms.1209

INTRODUCTION

Inclusion of electron correlation[1,2] in quantum chemical calculations is crucial for the correct description of chemical systems and their reactions. Especially interesting and, at the same time, particularly challenging for the existing theoretical methods are situations where the non-dynamic (or static) electron correlation plays the dominant role for the electronic structure.[3] Such situations are typically found in systems with dissociating chemical bonds, in low-spin states of biradicals, in excited states of molecules, in systems with anti-ferromagnetically coupled paramagnetic centers, and many more. In the domain of wavefunction theory (WFT), the accurate quantum chemical treatment of these situations is achieved by the use of multi-reference (MR) methods,[4] in which the static correlation effects are described by a superposition of several electronic configurations and the dynamic correlation effects are treated via many-body perturbation theory (PT),

*Correspondence to: mike.filatov@gmail.com

Institut für Physikalische und Theoretische Chemie, Universität Bonn, Bonn, Germany

Conflict of interest: The author has declared no conflicts of interest for this article.

coupled cluster (CC), or configuration interaction (CI) methods. Although the existing MR WFT approaches, such as the second-order complete active space PT (CASPT2),[5] MR singles and doubles CI (MRSDCI), MR CC with single and double substitutions (MRCCSD),[6,7] are capable of achieving a very high accuracy when predicting molecular properties, these methods are computationally quite involved and can be routinely applied to small and medium size molecular systems only.

The basic premise of the standard Kohn–Sham[8] (KS) density functional theory (DFT)[9] is that it should be capable of describing all pertinent correlation effects (dynamic and static) provided that the exact (i.e., yet unknown) exchange-correlation (XC) functional were employed. The existing approximations to the XC functional are designed to cover primarily the exchange (Fermi) and the dynamic electron correlation,[10] such as that which can be encountered in rare gas atoms or dense three-dimensional (3D) electron gas. However, the self-interaction error (SIE, residual self-repulsion of the electron) inherent in the exchange (major SIE) and the correlation (minor SIE) functionals lends approximate functionals the ability of providing for some implicit coverage of non-dynamic correlation effects.[11] Hence, covering both dynamic and static correlation effects (albeit the latter non-specifically, incompletely, and implicitly), approximate KS-DFT performs surprisingly well even in the situations that are notoriously difficult for the methods of WFT (e.g., ozone molecule).[12]

The implicit coverage of non-dynamic electron correlation by the approximate XC functionals, although beneficial for the description of the electronic structure of ordinary molecules near equilibrium geometry, becomes insufficient in situations typified by the strong static correlation. For example, this is manifested in the inability of the closed-shell KS-DFT to correctly describe the homolytic cleavage of a covalent bond or singlet-triplet energy splittings in organic biradicals. A simple remedy in the form of broken-symmetry (BS) spin-unrestricted KS-DFT (BS-UDFT or BS-UKS) has been widely used to describe the strongly correlated molecular systems, however, with alternating success. The BS-UKS approach introduces a certain degree of MR character via mixing states of different multiplicity (e.g., singlet and triplet states),[13,14] while retaining formally a single determinant KS reference state. The pertinent spin-contamination of the BS state, the high sensitivity of the calculated spin state energy differences on the employed approximate XC functional,[15,16] the necessity to employ a suitable mapping procedure to obtain the desired spin state energy[17,18] undermine the credibility of BS-UKS results for the electronic structure and properties of strongly correlated systems.

A potential remedy for shortcomings of the conventional KS DFT with regard to non-dynamic electron correlation is a merger between the MR methods of WFT (for treatment of non-dynamic correlation) with the correlation functionals of DFT (for treatment of dynamic correlation).[19–21] Although conceptually simple, the hybrid approach runs into the problem of double counting of electron correlation. Indeed, the static and dynamic correlation effects cannot be cleanly separated neither at the WFT level nor at the DFT level and, as a result of the merger, certain correlation effects are taken into account twice.[19,21,22] This becomes problematic for the correct description of multiplet states and energy splittings which may show strong and erratic dependence on the choice of the orbital active space in the MR WFT calculation.[21] Furthermore, the conventional approximate correlation functionals are designed to comply with the sum rules valid for single determinant states (or, equivalently, for idempotent density matrices)[23] and their use in connection with the densities from MR calculations [with fractional occupation numbers (FONs) of natural orbitals] was discouraged.[24] Although there was some initial success in designing the hybrid WFT/DFT schemes, the progress in this direction is relatively slow and no generally applicable hybrid scheme is available so far.

A different approach to the non-dynamic electron correlation is taken in ensemble DFT which goes beyond the widely accepted paradigm of KS-DFT that any physically meaningful fermionic ground state density can be uniquely mapped onto the ground state density of a fictitious system of non-interacting particles represented by a single KS determinant (the so-called pure-state V-representability, PS-VR).[8] In seminal works by Lieb,[25] Englisch and Englisch,[26,27] and later Kohn et al.[28] it has been rigorously proved that any ground state density is ensemble V-representable (i.e., representable by a weighted sum of several KS reference determinants, E-VR) and that only some physical densities are PS-VR. For a while, this notion remained a theoretical curiosity until it has been practically demonstrated, in a series of first principles simulations,[29,30] that mapping of the ground state density of certain molecular systems onto a non-interacting KS reference requires the use of ensemble representation which is manifested by the FONs of several frontier KS orbitals. And these were precisely the molecules in which the non-dynamic correlation becomes dominant.

The notion of using the fractionally occupied KS orbitals to simulate the non-dynamic correlation

in the context of KS DFT actually predates[12,31,32] the first rigorous theoretical work on this subject. The first attempts to implement the E-VR concept in the form of practically accessible DFT-FON have confronted the same difficulty as the WFT-DFT merger; namely, that the approximate XC functionals were not designed to comply with the fractional orbital occupations. The latter difficulty was circumvented by the notion that, if the same ensemble representation is used to construct both the density and the ground state energy of the strongly correlated molecule,[25] the standard approximate XC functionals can be used to calculate the energies of the individual ensemble components. This idea was implemented in the spin-restricted ensemble-referenced Kohn–Sham (REKS) method,[33] which was perhaps the first computationally feasible implementation of the E-VR concept. A considerable advantage of the REKS approach is that it enables one to study strongly correlated and ordinary (that is without strong non-dynamic correlation) molecular systems on the same theoretical footing, as the ensemble representation merely collapses to the single-reference (as in the conventional KS DFT) representation, if no strong non-dynamic correlation is present.

In the past, the REKS method has been successfully applied to investigate the electronic structure of strongly correlated molecular systems, such as the low-spin states of biradicals,[33–35] magnetically coupled metal centers,[36–38] organic charge transfer salts.[39,40] Later, the method has been extended to treat excited states of strongly correlated molecular species and the resulting state-averaged REKS (SA-REKS)[41] and state interaction SA-REKS (SI-SA-REKS)[42,43] methods have been used to investigate the photochemistry of molecular motors and molecular switches,[44–47] to study the excited states of extended π-conjugated molecules,[48] and to investigate peculiarities of the excited state charge transfer in donor–acceptor systems.[49] Although the REKS method has demonstrated its feasibility and ability to accurately describe fine detail of the electronic structure of strongly correlated molecular species, its theoretical background and practical implementation seem to be little known by the computational chemistry community at large. It is the purpose of this review article to bridge this gap and to provide an overview of the REKS method and its applications.

ENSEMBLE DFT AND REKS METHODOLOGY

Since its inception in the early 1960s, KS-DFT tacitly assumes that any physical fermionic ground state density $\rho(\vec{r})$ can be mapped onto the ground state density $\rho_s(\vec{r})$ of a fictitious system of non-interacting particles moving in a suitably modified external potential V_s, see Eq. (1)

$$\hat{H}_s = -\frac{1}{2}\sum_i \vec{\nabla}_i^2 + V_s(\vec{r}) \tag{1}$$

where the first term represents the kinetic energy operator of the non-interacting particles, $\hat{T}_s$. It is also assumed that such a $\rho_s(\vec{r})$ corresponds to a single Slater determinant (KS determinant) constructed from $N/2$ (N is the number of electrons; assumed to be even) lowest eigenfunctions of $\hat{H}_s$, see Eq. (2).

$$\rho_s(\vec{r}) = \sum_{i=1}^{N/2} 2\left|\phi_i(\vec{r})\right|^2 \tag{2}$$

The existence of such a non-interacting system and the corresponding potential can be demonstrated based on the adiabatic theorem of many-body physics.[50] Adiabatically switching off the electron–electron interaction $1/r_{ij}$ in the full many-body Hamiltonian $\hat{H}$,

$$\hat{H} = -\frac{1}{2}\sum_{i=1}^{N} \vec{\nabla}_i^2 + V_{ext}(\vec{r}) + \sum_{i>j}^{N} \frac{1}{r_{ij}} \tag{3}$$

where $V_{ext}(\vec{r})$ is the external potential (e.g., due to the nuclei), and modifying the external potential such that the ground state density remains unchanged[51] the non-interacting limit with the Hamiltonian (1) can be reached and the density obtained from its lowest eigenfunctions as in Eq. (2). Such an adiabatic connection path exists provided that (i) the many-electron system always remains in its ground state and (ii) the PT remains valid (i.e., there is a finite gap between the occupied and empty one-electron states) along the whole path. If such a potential V_s can be found, the ground state density constructed from its lowest eigenfunctions is said to be PS-VR.

The fact that not any physical fermionic density is non-interacting PS-VR has been theoretically proved already in the early days of KS DFT.[25–27] In the studies by Lieb,[25] Englisch and Englisch,[26,27] and later Ullrich et al.,[28] it was rigorously shown that the ensemble representation of the density is the only one that guarantees the existence of the KS potential V_s for any physical fermionic ground state density, that is any such density is E-VR and only some of the densities are PS-VR. E-VR implies that the density $\rho_s(\vec{r})$ can be represented as a

weighted sum (ensemble) of several KS determinants, that is

$$\rho_s(\vec{r}) = \sum_{L=1}^{M} \lambda_L \rho_L(\vec{r}),\ 0 \le \lambda_L \le 1,\ \sum_{L=1}^{M} \lambda_L = 1 \qquad (4)$$

a sum over a finite number (M) of ensemble components. In terms of the one-particle eigenfunctions of Eq. (1), the ensemble representation translates to the FONs of the orbitals ϕ_k and the density is given by Eq. (5),

$$\rho_s(\vec{r}) = \sum_{i=1}^{N/2} n_i \left|\phi_i(\vec{r})\right|^2,\ 0 \le n_i \le 2 \qquad (5)$$

where only a few KS orbitals are fractionally populated.

In spite of its formal exactness, the ensemble representation in DFT was considered a mere theoretical curiosity until the end of 1990s a series of works by Baerends and coworkers appeared,[24,29] where it was shown that the ensemble representation has a practical merit. These authors used the reverse engineering approach of Zhao-Morrison-Parr (ZMP)[52] for obtaining the KS potential V_s from known exact (or very accurate) density. For several strongly correlated systems, such as the C_2 molecule in its ground state near the equilibrium and at a slightly stretched bondlength,[29] and the $H_2 + H_2$ system in its ground state,[24] it was demonstrated that the FONs of several frontier orbitals (i.e., the ensemble representation) should be invoked in order to obtain physically meaningful potentials and precise mappings onto the target densities. A few years later, their conclusions were confirmed by Morrison,[30] who ran similar simulations on Be-like atomic ions. Taken together with the theoretical arguments (a recent development by Franck and Fromager[53] is to be added to this list), these findings have unambiguously demonstrated the practical relevance of the ensemble representation, which is the only rigorous representation for the density of a system with strong MR character.

REKS Method: General Setup

A practical implementation of ensemble DFT in the REKS method rests upon a rigorous statement that the energy of a strongly correlated system can be expressed, similar to its density (4), as a weighted sum over a finite number of the energies of the ensemble components, Eq. (6).[a]

$$E[\rho_s] = \sum_{L=1}^{M} \lambda_L E[\rho_L] \qquad (6)$$

To make use of Eq. (6) and to derive the expression for the REKS energy, let us consider a prototypal MR situation that arises in alkenes, such as ethylene, when twisting about the π-bond. At the planar conformation, the highest occupied molecular orbital (HOMO), let us denote it ϕ_a is doubly occupied and the lowest unoccupied orbital (LUMO), ϕ_b, is empty and there is a substantial energy gap between the orbitals and the corresponding electronic configurations, $\left(\ldots \phi_a^{(2)}\phi_b^{(0)}\right)$ and $\left(\ldots \phi_a^{(0)}\phi_b^{(2)}\right)$. The ground state of such a system can be accurately represented by a single KS determinant. When applying a torsion about the double bond (keeping the D_2 symmetry constraint, for simplicity), the gap between the two configurations narrows down and they become nearly degenerate at about 90° of twist, at which point the strong non-dynamic correlation ensues and the ground state density needs to be represented by an ensemble of the $\left(\ldots \phi_a^{(2)}\phi_b^{(0)}\right)$ and $\left(\ldots \phi_a^{(0)}\phi_b^{(2)}\right)$ densities. Thus, the non-interacting KS reference energy of such a system is to be given by a weighted sum over the KS energies of the two configurations taken with the weighting factors that are related to the FONs of the orbitals ϕ_a and ϕ_b, that is, $n_a/2$ and $n_b/2$. According to the exact KS simulations[24,29] and theoretical arguments[54] the fractionally occupied orbitals become degenerate and lie at the Fermi level of the system. The FONs of the orbitals are defined by the condition of stationarity of the KS energy with respect to the orbital population variations.[24,29,54]

Let us now follow the adiabatic connection path and turn the electron–electron interaction back on. At an infinitesimal coupling strength (consider a prefactor $\alpha \approx 0$ before the last term in Eq. (3)) only the two electrons occupying the fractionally populated (hence, degenerate) KS orbitals will be affected by the electron–electron interaction term. Applying the quasi-degenerate PT to calculate the energy of such a system leads to an expression

$$\begin{aligned} E[\rho_s] = {} & \frac{n_a}{2} E\left[\ldots \phi_a \overline{\phi}_a\right] + \frac{n_b}{2} E\left[\ldots \phi_b \overline{\phi}_b\right] \\ & + (n_a n_b)^{1/2} \left(\frac{1}{2} E\left[\ldots \phi_a \phi_b\right] - \frac{1}{2} E\left[\ldots \phi_a \overline{\phi}_b\right]\right. \\ & \left. + \frac{1}{2} E\left[\ldots \overline{\phi}_a \overline{\phi}_b\right] - \frac{1}{2} E\left[\ldots \overline{\phi}_a \phi_b\right]\right) \end{aligned} \qquad (7)$$

in which the bracketed term in the second line represents the negative of the exchange integral $(\phi_a\phi_b|\phi_b\phi_a)$ involving the fractionally occupied orbitals expressed via the energy differences between the singlet and triplet configurations with singly occupied frontier KS orbitals. Note that the bracketed term does not

contribute to the total density, as the densities of these configurations cancel each other identically. If no other degeneracies occur along the adiabatic path, it is plausible to assume that expression (7) will be valid at the full electron–electron interaction strength as well.

Equation (7) yields the energy of a system described by an E-VR reference state, for example, the ethylene molecule near 90° of twist about the double bond. For a system that is described by a single determinant KS reference state (PS-VR), the energy (7) should collapse to the usual DFT energy expression. Analyzing the dependence of the single reference KS DFT energy of the frontier orbital's FON's near $n_a \approx 2$ and $n_b \approx 0$, an expression similar to (7) can be obtained, with the only difference that the factor $(n_a n_b)^{1/2}$ is replaced by $(n_a n_b)^1$.[12,33] Thus, introducing a function $f(n_a, n_b)$ that interpolates between E-VR and PS-VR limits, one arrives at the working formula for the REKS (2,2) ground state energy, Eq. (8),

$$E^{\mathrm{REKS(2,2)}}\left[\rho_s\right] = \frac{n_a}{2}E\left[\ldots \phi_a\overline{\phi}_a\right] + \frac{n_b}{2}E\left[\ldots \phi_b\overline{\phi}_b\right] + f\left(n_a, n_b\right)\left(\frac{1}{2}E\left[\ldots \phi_a\phi_b\right] - \frac{1}{2}E\left[\ldots \phi_a\overline{\phi}_b\right] + \frac{1}{2}E\left[\ldots \overline{\phi}_a\overline{\phi}_b\right] - \frac{1}{2}E\left[\ldots \overline{\phi}_a\phi_b\right]\right) \quad (8)$$

where the function $f(n_a, n_b)$ is given by Eq. (9).

$$f\left(n_a, n_b\right) = \left(n_a n_b\right)^{1-\frac{1}{2}\left(\frac{n_a n_b + \delta}{1+\delta}\right)} \quad (9)$$

A damping factor δ in Eq. (9) is set to $\delta = 0.4$ to provide for a more stable convergence of the REKS self-consistent field (SCF) iterations when the E-VR solution (i.e., when $n_a \approx n_b \approx 1$) collapses to the PS-VR solution (i.e., when $n_a \approx 2$ and $n_b \approx 0$).[38] FONs of the frontier orbitals are constrained to sum up to two electrons, that is, $n_a + n_b = 2$. With the restriction to two active electrons in two fractionally occupied orbitals, Eq. (5) for the density becomes

$$\rho_s^{\mathrm{REKS(2,2)}}\left(\vec{r}\right) = \sum_i^{\mathrm{core}} 2\left|\phi_i\left(\vec{r}\right)\right|^2 + n_a\left|\phi_a\left(\vec{r}\right)\right|^2 + n_b\left|\phi_b\left(\vec{r}\right)\right|^2 \quad (10)$$

where all the KS orbitals but two are doubly occupied.

In Eq. (8), $E\left[\ldots \phi_a\overline{\phi}_a\right]$, etc., are the energies of single KS determinants constructed for the respective electronic configurations. As these are the single determinant configurations, the use of the approximate XC functionals for obtaining their energies is legitimate. Furthermore, the REKS(2,2) total energy is not obtained by substituting the ensemble density into an approximate density functional directly, which is known to lead to double counting of the non-dynamic electron correlation[21,22]; instead, an explicit account of this correlation is done via the ensemble formula, Eq. (8), which eliminates the double counting.[22] The outlined formalism for obtaining REKS energy and density is derived for a situation with two active electrons in two fractionally occupied orbitals. Such an active space is sufficient for describing a low-spin state of a biradical and a molecule with completely or partially dissociated bond. By analogy with *ab initio* MR WFT, this version of the REKS method is denoted REKS(2,2) which implies its similarity (however, not an equivalence) to the respective CASSCF method.

REKS Method: One-Electron Equations

The REKS total energy is minimized with respect to the REKS orbitals and FONs of the active orbitals. Strictly speaking, such a minimization does not result in a local multiplicative potential V_s as in Eq. (1). However, for obtaining such a potential it would be necessary to employ a variant of the optimized effective potential (OEP) approach, which is known to suffer from steep computation time scaling and certain stability issues when used in connection with the localized basis sets for expanding the KS orbitals.[55] Therefore, one typically resorts to optimizing the total energy with respect to the orbitals, as is being commonly done in connection with the hybrid and meta generalized gradient approximation (GGA) density functionals, thus avoiding the necessity to handle with the density–density response function.

Varying the REKS total energy (8) (which for the sake of convenience is represented in the form of Eq. (6) with the respective weighting factors) with respect to the orbitals, one arrives at a set of one-electron equations

$$\begin{aligned}\widehat{F}_k\phi_k &= \sum_l^{\mathrm{core}}\phi_l\,\varepsilon_{lk} + \sum_w^{\mathrm{act}}\phi_w\,\varepsilon_{wk};\ k \in \mathrm{core}\\ f_v\,\widehat{F}_v\phi_v &= \sum_l^{\mathrm{core}}\phi_l\,\varepsilon_{lv} + \sum_w^{\mathrm{act}}\phi_w\,\varepsilon_{wv};\ v \in \mathrm{act}\end{aligned} \quad (11)$$

in which ε_{qp} are the Lagrange multipliers that carry out the orbital orthogonality constraints, the orbitals ϕ_q are labeled by the indices l, k when they belong in the core (doubly occupied orbitals) and by v, w when they belong in the fractionally occupied active orbitals (ϕ_a and ϕ_b in Eqs. (8) and (10)), $f_v = n_v/2$, and the one-electron KS operators $\widehat{F}_q$ ($q \in \{\mathrm{core}, \mathrm{act}\}$) are given by Eq. (12)

$$\widehat{F}_q = n_q^{-1}\sum_L \lambda_L\left(n_{q,L}^{\alpha}\widehat{F}_L^{\alpha} + n_{q,L}^{\beta}\widehat{F}_L^{\beta}\right) \quad (12)$$

in which λ_L are the respective weighting factors, cf Eqs. (6) and (8), of the single determinant configurations (microstates), $n^{\alpha}_{q,L}$ and $n^{\beta}_{q,L}$ are the populations of the respective spin-orbitals in the microstate L (0 or 1), and $\widehat{F}^{\alpha}_{L}$ and $\widehat{F}^{\beta}_{L}$ are the usual KS operators for the α and β spin-orbitals of the respective microstates. The weighting factors λ_L are repeated for convenience in Eq. (13),

$$\lambda_1 = \frac{n_a}{2};\ \lambda_2 = \frac{n_b}{2};\ \lambda_3 = -\lambda_4 = \lambda_5 = -\lambda_6 = \frac{1}{2} f\left(n_a, n_b\right) \tag{13}$$

where they are given in the order of their appearance in Eq. (8).

Although the one-electron equations (11) look similar to the usual KS (or HF) equations, they cannot be solved by applying recurrent diagonalization as is being typically done when solving the closed-shell or spin-unrestricted open-shell KS equations. At the variational minimum of the REKS energy, the matrix of the Lagrange multipliers becomes Hermitian, that is, $\varepsilon_{pq} = \varepsilon^{*}_{qp}$, or in terms of the one-electron operators (12)

$$\langle p | n_q \widehat{F}_q | q \rangle = \langle p | n_p \widehat{F}_p | q \rangle \tag{14}$$

and—because the energy within the spin-restricted open-shell formalism is not invariant with respect to orthogonal transformation of the core and active orbitals—this matrix should not be diagonalized. The one-electron equations (11) are thus solved by the use of the coupling operator technique of Hirao and Nakatsuji[56] which provides for obtaining the true variational minimum of the REKS energy at a typical mean-field cost. Note however that, due to arbitrariness in the choice of the diagonal Lagrange multipliers in the open-shell SCF theory,[57] the REKS Lagrange multipliers ε_{pp} do not obey Koopmans' theorem and do not represent good approximations to the ionization potentials of the respective orbitals.

Minimization of the REKS energy (8) with respect to the FONs of the active orbitals is carried out at each SCF iteration by applying a Newton–Raphson technique and a constraint $n_a + n_b = 2$. Under the latter constraint, the REKS energy is to be minimized with respect to the FON of a single active orbital, which leads to the following equation

$$\frac{\partial f(x)}{\partial x} + \frac{\partial^2 f(x)}{\partial x^2}\left(x_{\min} - x\right) = \frac{2\left(E_{a\bar{a}} - E_{b\bar{b}}\right)}{E_{ab} - E_{a\bar{b}} + E_{\bar{a}\bar{b}} - E_{\bar{a}b}} = \Delta \tag{15}$$

solved iteratively for the value of $x = n_a/2$ that minimizes the REKS energy at the current iteration (in practical calculations, ϕ_a is always the strongest populated active orbital). In Eq. (15), the function $f(n_a, n_b)$ of Eq. (9) is written utilizing the variable x and the above constraint on the active orbital's FONs. Figure 1 shows the optimal value of the variable x as a function of the right-hand side of Eq. (15) obtained for several values of the damping factor δ of Eq. (9). It is seen that, for $\delta \approx 0.4$ or greater, the dependence of the active orbital's FONs (as given by x) on the ratio Δ of the energy gap between the $\left(\ldots \phi_a^{(2)} \phi_b^{(0)}\right)$ and $\left(\ldots \phi_a^{(0)} \phi_b^{(2)}\right)$ microstates and the effective exchange integral $-\left(\phi_a\phi_b|\phi_b\phi_a\right) \approx \left(E_{ab} - E_{a\bar{b}} + E_{\bar{a}\bar{b}} - E_{\bar{a}b}\right)/2$ (that defines coupling between the former microstates) becomes smooth and does not cause any instability of the iterative solution of the one-electron equations (11).

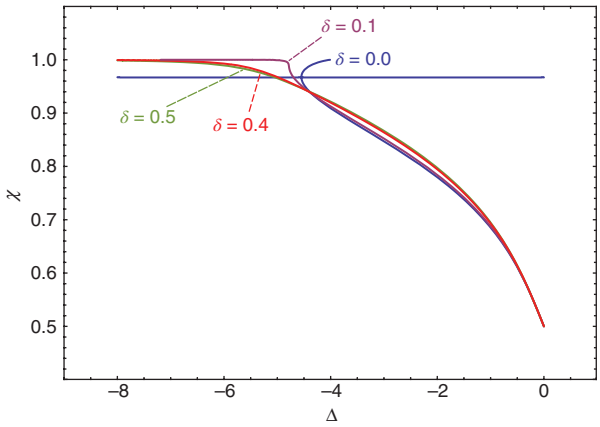

FIGURE 1 | Optimal value of the parameter $x = n_a/2$ as a function of the ratio Δ on the right-hand side of Eq. (15).

The described SCF approach to solving the REKS equations does not yield canonical Lagrange multipliers that can be interpreted as the one-electron energies in the same sense as it is done in the case of closed-shell single-reference systems. However, had these Lagrange multipliers been obtained when minimizing the REKS energy, the one-electron energies of the active electrons (that is electrons in the fractionally occupied frontier orbitals) would be exactly degenerate, because the total REKS energy is stationary with respect to FONs of the active orbitals.[54] Obtaining such one-electron energies would however require imposing an additional constraint for the number of particles conservation,[54] which could make the self-consistent solution of the REKS one-electron equations more time consuming and was therefore avoided when deriving these equations.

For automatic search for local stationary points on the molecular potential energy surfaces (PESs) the analytic energy gradient is available for the REKS

method. The derivation is straightforward and results in the following general formula for the derivative of the total REKS energy with respect to an external perturbation X (atomic displacement, external field, etc.),[33]

$$\frac{\partial E^{\mathrm{REKS}}}{\partial X} = \sum_L \lambda_L \frac{\partial' E_L}{\partial X} + \sum_{p,q}^{\mathrm{occ}} \left(\langle p|n_p \hat{F}_p|q\rangle + \langle p|n_q \hat{F}_q|q\rangle \right)^s U^X_{qp} + \sum_{p,q}^{\mathrm{occ}} \left(\langle p|n_p \hat{F}_p|q\rangle - \langle p|n_q \hat{F}_q|q\rangle \right)^a U^X_{qp} \quad (16)$$

where E_L are the energies of the individual microstates in Eq. (8) and λ_L are their weighting factors, Eq. (13), the prime at the differentiation symbol implies that only the molecular integrals over the basis functions (and not the density matrix elements) have to be differentiated, and ${}^sU^X_{ji}$ and ${}^aU^X_{ji}$ are the symmetric and antisymmetric parts of the orbital response matrix, where the former is (C is the matrix of the KS orbital coefficients and S is the matrix of the overlap integrals between the basis functions)

$${}^sU^X = -\frac{1}{2} C^\dagger \frac{\partial S}{\partial X} C \quad (17)$$

and the latter is to be obtained with the use of the coupled-perturbed formalism. As the REKS orbitals are obtained self-consistently and satisfy the variational conditions in Eq. (14), the last term in Eq. (16) vanishes and the REKS gradient can be obtained through the derivatives of the molecular integrals only, which has the same cost as in a conventional KS calculation. The expression in Eq. (16) however is also valid for situations when non-self-consistent orbitals are used to calculate the REKS energy, as in the SA-REKS and SI-SA-REKS methods to be described later on.

REKS Method: Prospects of Extension

Further development of the REKS method will require extension of its active space to include more electrons and fractionally occupied orbitals. Such an extension can be achieved by the same argument as was used when deriving Eq. (7), i.e., starting from a system of non-interacting particles and employing the quasi-degenerate PT. In this way, the energy expression for the (2,m) active space (m is the number of fractionally occupied orbitals) can be derived by retaining only doubly excited electronic configurations with both electrons excited to the same orbital. The coupling matrix elements between these configurations can be obtained similar to Eq. (7) as the energy differences between singly excited singlet and triplet electronic configurations. As the fractionally occupied orbitals are variationally optimized, the energy contribution of the singly excited configurations is introduced via the orbital optimization. By exploiting the particle-hole symmetry, the energy expression for the ($2m$-2,m) active space can be obtained. The orbital optimization scheme for described extension of REKS has not yet been implemented and only non-self-consistent calculations have been carried out for a few model systems with (2,3) and (4,3) active spaces, which shown feasibility of the method.

With the setup described above the number of free variables in REKS (the FONs of active orbitals) is the same as the leading dimension of the secular problem ($m \times m$) resulting from the application of quasi-degenerate PT. The further extension of REKS to (4,4), (6,6), etc. active spaces will require a certain reduction of the secular problem resulting from PT, as there are fewer fractionally occupied orbitals than the dimension of the secular problem. This implies that there is no simple relationship between the FONs and the eigenvectors of the secular problem, which may complicate the derivation of the total energy expression. To bypass this problem, a model approach similar to the one used in generalized valence bond method[58] can be used, namely restricting possible double excitations to dedicated orbitals pairs. The feasibility of such a method has not yet been assessed.

ILLUSTRATIVE APPLICATIONS OF REKS METHOD

The REKS methodology outlined in the preceding section is suitable for describing chemical systems in which homolytic bond breaking/bond formation processes occur, such as dissociation of a chemical bond, avoided crossing of several electronic configurations, as well as systems with loosely coupled unpaired electrons, such as biradicals. Computational modeling of these situations is also possible with the use of the BS-UKS approach; however, in this case one has to deal with the excessive spin-contamination that results from mixing of the states of different spin-multiplicity, e.g., a singlet and a triplet. By contrast, the REKS method is free of this drawback and enables one to unambiguously describe the true singlet states of strongly correlated molecular systems. In the following, several illustrative examples of application of the REKS method to the aforementioned chemical systems will be presented. The purpose of this presentation is to give the reader an idea of what can be done with the use of REKS and not to provide for an exhaustive review of its applications.

Bond Dissociation

Perhaps the simplest situation where the strong non-dynamic correlation can be met in chemistry is the situation of a dissociating chemical bond. Depending on the relative electronegativity of the fragments the cleavage can occur by a heterolytic mechanism, when both electrons in the bond are shifted toward the more electronegative fragment, or by a homolytic mechanism, when the electron pair is equally split between the fragments. In the latter case, the ground state of the system is dominated by a configuration with two loosely coupled electrons localized on the opposite ends of the dissociating bond.

A paradigmatic example of bond cleavage is the dissociating dihydrogen molecule.[33] Near the equilibrium interatomic distance R_{HH} (0.74144 Å,[67] 1.401 bohr[59]) the ground state of the molecule is dominated by the $(1\sigma_g)^2$ electronic configuration with the doubly occupied totally symmetric MO that can be described as the in-phase superposition of the hydrogen atomic orbitals (AOs). Along the H–H bond stretching coordinate, the doubly excited electronic configuration $(1\sigma_u)^2$ with the doubly occupied antibonding MO becomes lower in energy, as the overlap between the AOs decreases, and at some interatomic separation (known as the Coulson–Fischer point)[60] the energy gap between the two electronic configurations narrows down to a limit that allows for an efficient mixing of the configurations and the strong non-dynamic electron correlation ensues.[33] Referring to the plot in Figure 1, the strong non-dynamic correlation sets in when the absolute value of the ratio Δ defined in Eq. (15) becomes smaller than ca 4 and the population of the bonding $1\sigma_g$ orbital deviates noticeably from 2 electrons.

Figure 2 compares the ground state potential energy curves obtained using the CC with single and double substitutions (CCSD), the usual single-reference spin-restricted KS (RKS) method, the BS-UKS, and the REKS(2,2) methods in connection with the cc-pV5Z basis set modified as in Ref 24. The DFT calculations employ the range-separated CAM-B3LYP functional.[61] For a molecule with only two electrons, such as H_2, the CCSD method is equivalent to full configuration interaction (FCI) approach. Figure 2 also shows the population of the bonding orbital of H_2 obtained from analysis of the density matrix (relaxed density matrix in the case of CCSD) Note however, that the natural orbital's occupation numbers (NOONs) obtained for the correlated WFT or the BS-UKS methods are not fully equivalent to the FONs of the frontier orbitals in the ensemble KS theory. Generally, the NOONs are non-integer for all orbitals in the molecule (some closer to 2, some closer to 0), while the FONs are allowed to be non-integer for a few frontier orbitals only; for the case of dissociating H_2, the bonding $1\sigma_g$ and the antibonding $1\sigma_u$ MOs.

The single-reference RKS method is well known to fail to describe the homolytic bond dissociation correctly and, at long interatomic separations, it approaches a wrong dissociation limit, a 50–50 mix of ionic and covalent electronic configurations.[60] REKS and BS-UKS describe the dissociation correctly; however, the switch over from the PS-VR solution near the equilibrium H–H distance and the E-VR solution at the stretched bond occurs abruptly in the case of BS-UKS method (see the BS-UKS NOON plot near $R_{HH} = 2.8$ bohr in Figure 2), while REKS describes a smooth transition between the two

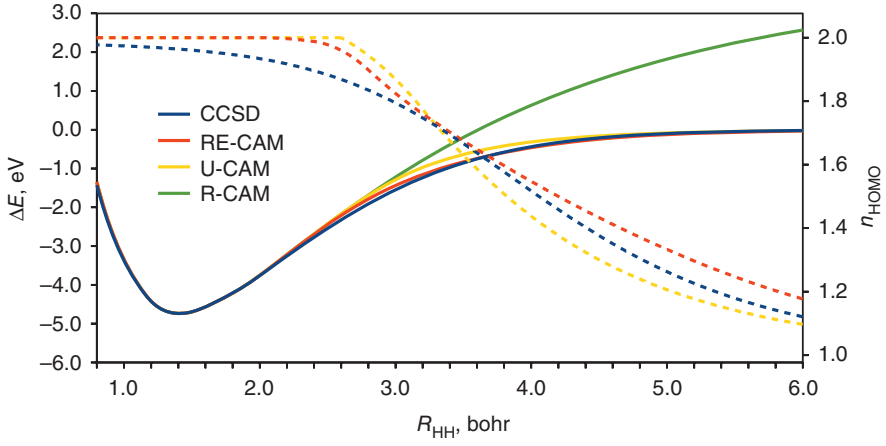

FIGURE 2 | Dissociation curve of the H_2 molecule in the $^1\Sigma_g^+$ ground electronic state as obtained using the REKS(2,2) (red), RKS (green), BS-UKS (yellow), and CCSD (blue) methods. The solid curves refer to the relative energy with respect to the dissociation limit of two neutral atoms, the dashed curves refer to the population of the $1\sigma_g$ bonding orbital (HOMO) obtained as the natural orbital population for the respective method.

regimes.[33] The sudden onset of the non-dynamic correlation as described by BS-UKS may result in discontinuities of the PES when one applies an *a posteriori* spin-purification scheme,[62,63] see e.g., Figure 1 of Ref 63. It is also noteworthy that the BS-UKS energy curve deviates stronger from the exact (CCSD) curve than the REKS energy curve in the region where the transition between the single-reference and MR situation occurs, between ca 2.8 and 4.2 bohr. The XC functional derived from the random phase approximation (RPA) was demonstrated to be capable of producing the correct dissociation limit for H_2.[64] Being computationally more demanding than REKS, the RPA XC functional yields an unphysical hump (ca 1 eV) at the intermediate distances[64,65]; the behavior that can be corrected only by using the considerably more expensive approach based on solving the Bethe-Salpeter equation of many-body physics.[65]

A more interesting situation occurs during dissociation of an ionic bond, such as the σ-bond in LiH.[66] Near the equilibrium bondlength (1.5957 Å)[67] the electronic structure of lithium hydride molecule is dominated by a $Li^{\delta+}$–$H^{\delta-}$ electronic configuration which corresponds to the doubly occupied σ-type bonding MO. Figure 3 shows the LiH dissociation curves obtained using the CCSD (the 1s electrons of Li were put into the frozen core), BS-UKS, RKS, and REKS methods in connection with the cc-pV5Z basis set[24] and CAM-B3LYP functional. Along with the energy curves, the variation of the Mulliken charge on Li is shown as a function of the interatomic distance. Near the equilibrium distance, there is a substantial transfer of charge (ca 0.4 e) to the hydrogen atom. As the Li–H bond dissociates, the charge is back transferred to Li and, at the dissociation limit, the ground state is dominated by a biradical (covalent) valence configuration $Li^{\bullet}$–$H^{\bullet}$. The transition between the ionic and covalent electronic configurations is described by the REKS and BS-UKS methods qualitatively correctly, as displayed in the energy and charge curves in Figure 3. Similar to the hydrogen molecule case, BS-UKS describes an abrupt transition between the closed shell (ionic) and open-shell (covalent, biradical) electronic configurations, as can be seen in the charge curve near $R_{LiH} = 5.5$ bohr in Figure 3. The single-reference RKS method fails to describe the Li–H bond dissociation properly and, at the limit of dissociated bond, it yields an ionic configuration with $Q_{Li} = 0.43$ e.

The presented examples demonstrate the ability of REKS to take proper account of non-dynamic correlation during dissociation of a single chemical bond.[33] It is gratifying that near the equilibrium geometry, REKS yields the same total molecular energy as the single-reference RKS approach. This implies that, for molecules correctly described by the standard single-reference KS DFT, the REKS method avoids double counting of the non-dynamic correlation, which plagues the approaches based on merging MR WFT with DFT.

The described bond dissociation situations may not seem particularly interesting when only the ground electronic state is addressed. It becomes more difficult (and, for BS-UKS, nigh impossible) to describe the excited states of a molecule that undergoes bond dissociation. However, REKS formalism is capable of providing a correct and accurate description of such systems, which will be discussed later on. For now, let us continue with the molecular ground state and

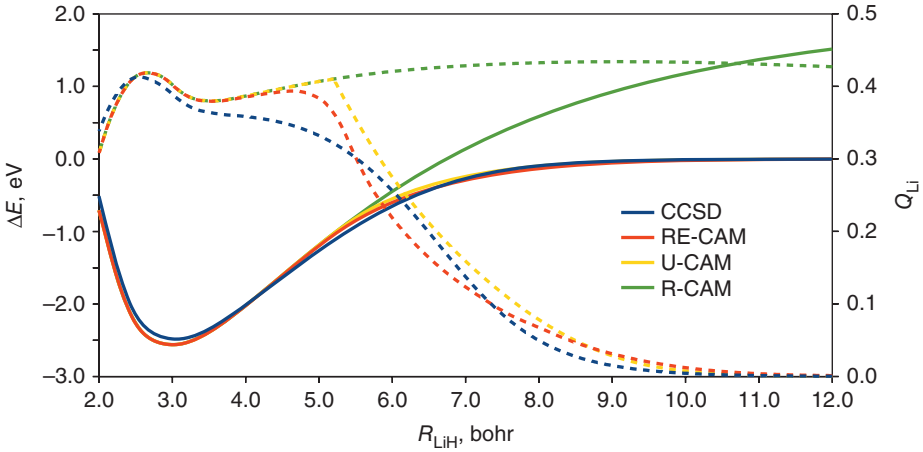

FIGURE 3 | Dissociation curve of the LiH molecule in the $^1\Sigma^+$ ground electronic state as obtained using the REKS(2,2) (red), RKS (green), BS-UKS (yellow), and CCSD (blue) methods. The solid curves refer to the relative energy with respect to the dissociation limit of two neutral atoms, the dashed curves refer to the Mulliken charge on Li atom.

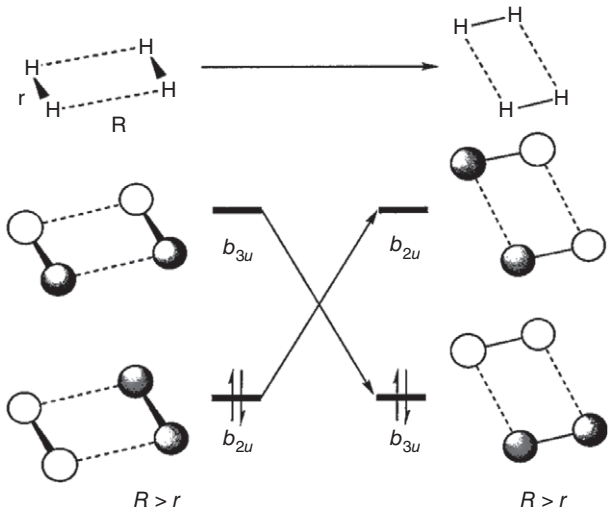

SCHEME 1 | Geometric parameters and frontier orbitals of $H_2 + H_2$ system. (Reprinted with permission from Ref 34 Copyright 2000 American Chemical Society)

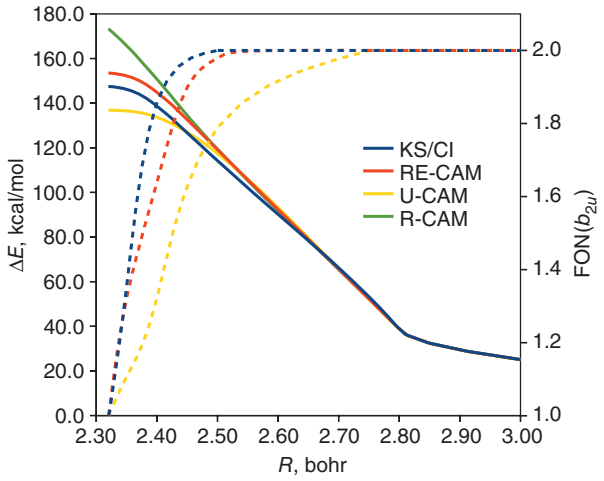

FIGURE 4 | Profile of the PES of $H_2 + H_2$ reaction and populations of the b_{2u} orbital as obtained from the KS/CI[24] (blue), BS-UKS (yellow), RKS (green), and REKS (red) calculations. The relative energies are calculated with respect to two isolated H_2 molecules. Solid curves show the energies and dashed curves show the occupation numbers as a function of R (see Scheme 1 for definition). DFT calculations employ the CAM-B3LYP functional.

discuss systems where avoided crossing of electronic configurations takes place.

Avoided Crossings

Situations of avoided crossing typically occur in symmetry forbidden reactions such as electrocyclic reactions and cycloadditions.[68–70] At some point along the reaction coordinate, the excited electronic configuration becomes near degenerate with the ground state configuration and that leads to a significant activation barrier of the reaction.[68–70] Perhaps the simplest example of such a process is the 2+2 cycloaddition of two H_2 molecules which has been investigated at the MRSDCI level of theory using large cc-pV5Z basis set.[24] Along the rectangular reaction mode (D_{2h} point group) shown in Scheme 1 crossing between the $(\ldots b_{2u}{}^2 b_{3u}{}^0)$ and $(\ldots b_{2u}{}^0 b_{3u}{}^2)$ electronic configurations occurs at an approximately square geometry of H_4. This results in a strong mixing between the two electronic configurations near the transition state for this reaction mode and to an avoided crossing between the ground and doubly excited states. For this system, the exact KS solutions have been obtained in Ref 24 starting from the MRSDCI density and it was unambiguously demonstrated that one has to switch to the ensemble representation for the KS reference near the square geometry of H_4. From the exact KS/CI simulations of Ref 24 the FONs of the frontier (b_{2u} and b_{3u}) orbitals are available and are shown in Figure 4 along with the energy profile along the reaction coordinate.

The PES profile and the FONs obtained[34] with the REKS, BS-UKS (NOON is used in lieu of FON), and RKS calculations are compared in Figure 4 with the results of the exact KS/CI calculations.[24] The single-reference RKS approach is not capable of taking proper account of the non-dynamic correlation near the top of reaction barrier and yields a cusp on the PES instead of a smooth transition between the $(\ldots b_{2u}{}^2 b_{3u}{}^0)$ and $(\ldots b_{2u}{}^0 b_{3u}{}^2)$ electronic configurations. The BS-UKS and REKS methods yield a smooth transition between the two configurations; however, the BS-UKS PES deviates stronger from the exact (MRSDCI) one and the reaction barrier is underestimated, which is typical for this approach. According to BS-UKS, the non-dynamic correlation sets in abruptly, after ca $R = 2.75$ bohr, and the NOON of the b_{2u} orbital deviates noticeably from the exact KS/CI FON indicating certain overestimation of the non-dynamic correlation by BS-UKS. By contrast, REKS yields a smooth onset of the non-dynamic correlation (as seen from the FON curve in Figure 4) and provides a more accurate description of the reaction barrier.

Yet another situation of avoided crossing of the ground and excited states occurs in alkenes, such as ethylene, when torsion about the double bond is involved.[33,34] The ground electronic state of ethylene near its equilibrium geometry can be sufficiently accurately described by the $(\ldots b_{3u}{}^2 b_{2g}{}^0)$ configuration where the π-bonding MO (b_{3u}) is doubly occupied and the π^*-antibonding MO (b_{2g}) is empty. When torsion about the double bond reaches near 90° of twist, the doubly excited electronic configuration $(\ldots b_{3u}{}^0 b_{2g}{}^2)$ becomes near degenerate with the

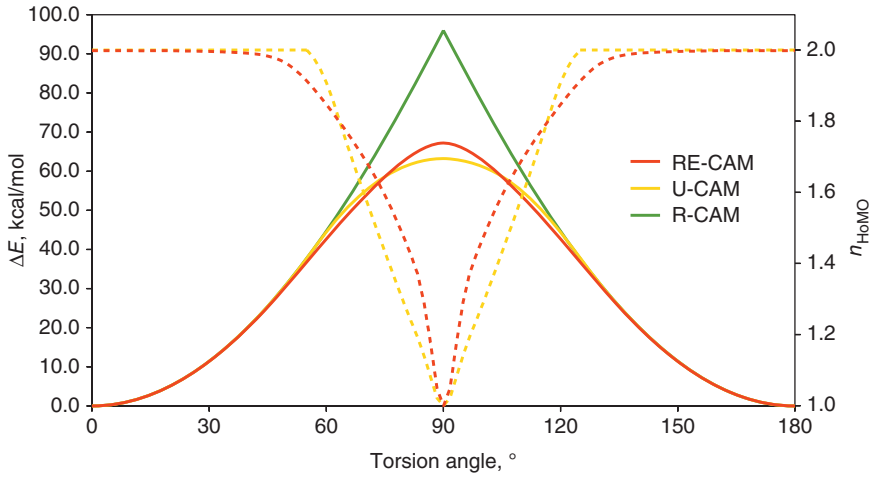

FIGURE 5 | Profile of the ground state PES of ethylene along the π-bond torsion mode. The energies (solid curves) and the populations of the b_{3u} orbital (dashed curves) as obtained by the BS-UKS (yellow), RKS (green), and REKS (red) methods are shown. The relative energies are calculated with respect to the planar conformation. The cc-pVTZ basis set is employed in connection with the CAM-B3LYP density functional.

($\ldots b_{3u}{}^2 b_{2g}{}^0$) configuration and this leads to a strong mixing of the two configurations in the ground state which acquires MR character.

With the use of single-reference RKS method, the mixing between the configurations and the non-dynamic correlation in the ground state of twisted ethylene molecule cannot be described at all and the RKS method yields a cusp on the ethylene PES at 90° of torsion, see Figure 5. The REKS and BS-UKS methods capture the non-dynamic correlation; however, BS-UKS describes the onset of MR state at ca 50° of torsion abruptly as can be judged from the b_{3u} orbital NOON, which begins suddenly deviate from the closed-shell value of 2 (Figure 5). REKS describes the transition between the single-reference PS-VR state and the MR E-VR state smoothly and yields a somewhat higher torsion barrier (67.2 kcal/mol) than BS-UKS (63.2 kcal/mol). From the b_{3u} population curves in Figure 5 it can be seen that BS-UKS populations deviate noticeably from the REKS ones for the intermediate torsion angles. Likely, this is caused by the spin contamination of the BS-UKS reference wavefunction due to mixing singlet and triplet electronic configurations.

Some other examples of application of the REKS method to description of avoided crossings can be found in the literature.[34,71] Together with the aforementioned systems, they confirm that REKS is capable of accurately describing avoided crossings and can be used with confidence to study symmetry-forbidden reactions. A number of chemically relevant examples of the calculation of the ground and excited states of symmetry-forbidden reactions will be presented later on, when discussing the SA-REKS and SI-SA-REKS methods. In the next subsection, however, let us briefly review application of REKS to another interesting situation, the low-spin states of biradicals.

Biradicals and Magnetic Coupling

Molecules with two unpaired and loosely coupled electrons are commonly known as biradicals (or diradicals). Typically, biradicals have low lying singlet and triplet electronic states either of which may happen to be their ground state.[72] However, as the singlet–triplet (ST) gap is sufficiently narrow, quite often the upper state can be thermally populated as well. In this way, the physical properties and reactivity of biradicals, which may often occur as intermediates of chemical reactions, are defined by the magnitude of the ST energy gap.

The REKS method has been applied to study the ST splitting in a wide range of biradicals, including organic molecules and metal complexes.[33–38] It was found to be more reliable than the commonly employed BS-UKS methods, especially when the ST gap is substantially large, on the order of a few kcal/mol or more.[22] Naturally, the spin-restricted open-shell KS (ROKS) method is to be used for computing the triplet state in connection with REKS for the singlet. Using the spin-restricted methods for modeling both the singlet and the triplet helps to avoid the erroneous spin-contamination inherent in the spin-unrestricted methods, such as UKS and BS-UKS. However, the results of REKS/ROKS calculations of the ST gaps were found to be sensitive to the choice of the XC functional, though perhaps to a somewhat lesser extent than BS-UKS ones,[36–38] mainly due to the SIE of density functionals.[22] It was thus recommended to mitigate the SIE as much as possible and to employ the hybrid density functionals with sufficiently large

fraction of the exact exchange. As the REKS method reproduces the results of the conventional RKS calculations for the ordinary (i.e., not strongly correlated) molecular systems, the benchmarks of the XC functionals carried out at the RKS level may serve as a guidance when choosing a functional for the REKS calculations. Typically, BH&HLYP, CAM-B3LYP and similar XC functionals provide for a balanced description of the static and dynamic correlation effects in the context of the REKS method.

To illustrate the performance of REKS in the calculation of ST gaps in biradicals, the results of the calculations of a series of didehydrobenzene biradicals (or benzynes) are reported here. More results on various organic biradicals and binuclear copper complexes can be found in the original publications.[22,33–38] The reported here ST gaps in the ortho- (**1**), meta- (**2**), and para-benzyne (**3**) are obtained using the range-separated hybrid CAM-B3LYP functional in connection with the cc-pVTZ basis set and the geometries optimized for the respective computational method.

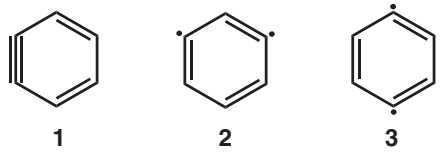

1 **2** **3**

Table 1 compares the REKS/ROKS and BS-UKS/UKS ST energy gaps for **1**, **2**, and **3** with the theoretical results and experimental data available in the literature.[73–75] Compared to the golden standard of current computational chemistry, the CCSD(T) method, REKS/ROKS formalism is coming out quite well both in terms of the ST energy splittings and the diradical character (the latter was evaluated from the population of the weakly fractionally populated frontier orbital).[22] The BS-UKS approach strongly overestimates the diradical character of m- and p-benzynes; however, yields a closed-shell configuration for the ground singlet state of o-benzyne. The absolute magnitude of the ST energy gaps of benzynes is underestimated by the BS-UKS/UKS approach; for m-benzyne by almost a factor of two as compared to CCSD(T), see Table 1.

Another interesting application of the REKS method worth mentioning is establishing the shape of the PESs of the lowest singlet and triplet states of tetramethyleneethane (TME) biradical.[35] TME is a disjoint, non Kekulé diradical, the electronic structure of which is dominated by two resonance structures shown Scheme 2. Depending on the coupling between the unpaired electrons, TME may exist in the triplet or the singlet ground state.

TABLE 1 | Singlet-Triplet Energy Gap (kcal/mol) in Benzyne Biradicals

Method	o-Benzyne	m-Benzyne	p-Benzyne
REKS/ROKS[1]	32.3 (8)[2]	15.9 (33)	3.1 (61)
BS-UKS/UKS[1]	29.8 (0)	9.9 (46)	2.3 (80)
CCSD(T)[3]	35.1 (11)[4]	17.1 (20)	3.1 (65)
Exp.[5]	37.5 ± 0.3	21.0 ± 0.3	3.8 ± 0.3

[1] DFT calculations employ CAM-B3LYP functional and cc-pVTZ basis set.
[2] Diradical character (%) is given in parentheses.
[3] CCSD(T)/cc-pVTZ results from Ref 73.
[4] CCSD(T) diradical character from Ref 74.
[5] Gas phase experimental enthalpy differences from Ref 75.

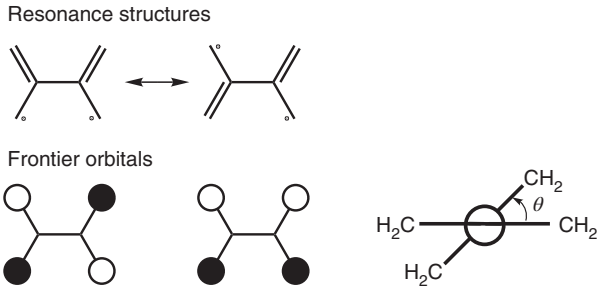

SCHEME 2 | TME biradical.

The REKS/ROKS calculations[35] predicted that the preference for either triplet or singlet state depends on the torsion angle ϑ (see Scheme 2) and that, at an intermediate torsion angle $\vartheta \approx 45°$, the triplet becomes TME's ground state, while, at the orthogonal orientation of the two allyl fragments, the ground state becomes singlet (see Figure 6). Qualitatively, this assignment is supported by the experimental EPR measurements, which yield a linear Curie-Weiss temperature dependence of the EPR intensity,[76] and by recent quantum Monte-Carlo (QMC) calculations, which predict that the triplet becomes a metastable ground state at an intermediate torsion angle. As was recently analyzed by Borden et al.[77] the metastable character of triplet TME, which is slowly decaying to singlet under the experimental conditions, is the only way to reconcile the observation of its magnetism and the results of the negative ion photoelectron spectroscopy that unambiguously put the singlet state below the triplet.[78]

To round up this section, the REKS method has proved its ability to provide qualitatively and quantitatively accurate description of various strongly correlated molecular systems. An advantage of REKS methodology, especially before the approaches based on merging MR WFT with density functionals specifically designed to match the WFT part,[21] is that the method can be used in connection with any existing pure or hybrid density functional, including the dispersion corrected functionals.[79,80] Besides that, the

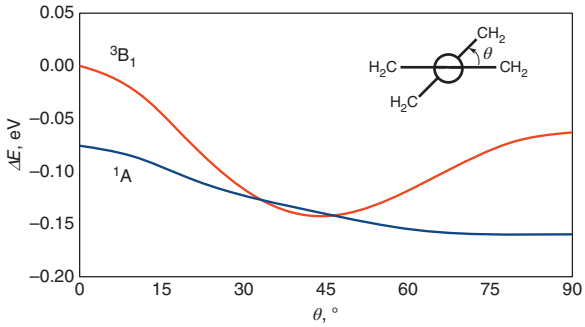

FIGURE 6 | Relaxed potential energy curves of TME diradical along the torsion mode ϑ. The REKS/ROKS calculations are carried out using the CAM-B3LYP density functional in connection with the cc-pVTZ basis set.

REKS method does not suffer from effects of the erroneous spin-contamination, which plagues the BS-UKS approach and undermines its credibility. Although the application of REKS to strongly correlated molecular species offers a theoretically sound and numerically accurate way of analyzing their ground state electronic structure and reactivity, the greatest advantage of the REKS formalism is in its ability to accurately describe the excited states of these species, which are beyond the reach of the most popular computational approaches in the domain of DFT. Application of the REKS formalism to excited states will be reviewed in the following section.

REKS METHODOLOGY FOR EXCITED STATES

Presently, the most popular approach to excited states in the framework of DFT is the linear-response time-dependent DFT (TD-DFT) in which the excitation energies are obtained from the poles of the density–density response function.[81] Despite its popularity, TD-DFT experiences well-known difficulties with describing certain types of excitations, which include charge transfer excitations, double excitations, and excitations of a system with strongly correlated ground state.[82] There have been proposed a number of remedies to cure these deficiencies of TD-DFT,[83] in particular, going beyond the linear response approximation was put forward as the way to improve the description of charge transfer excitations.[84,85]

An alternative to using the density response to obtain the excitation energies is in the use of ensemble formalism. The ensemble DFT formalism has been extended to the domain of excited states by Gross, Oliveira, and Kohn (GOK)[86] who proved the applicability of the variational principle—and hence the existence of the Hohenberg-Kohn theorem, that is the exact mapping of the ensemble density of the type (4) onto the external potential V_{ext}—for ensembles of ground and several excited states (as in Eq. (6) but for *interacting* states). In this way, the GOK approach represents a continuation of the line of research set out by Lieb[25] and Englisch and Englisch.[26,27] For instance, considering an ensemble of the ground E_0 and a single excited E_1 states with the energy and density given by

$$E_\omega = (1-\omega)\,E_0 + \omega E_1\ ;\ 0 \le \omega \le 1 \tag{18}$$

$$\rho_\omega(\vec{r}) = (1-\omega)\,\rho_0(\vec{r}) + \omega\rho_1(\vec{r}) \tag{19}$$

and variationally minimizing the energy E_ω with respect to the density ρ_ω one obtains the excitation energy ΔE_{12} from Eq. (20).[81]

$$\Delta E_{12} = \frac{E_\omega - E_0}{\omega} \tag{20}$$

Although it rests on a rigorous physical foundation,[53,81,86] until recently, this formalism was not developed into a useful practical computational scheme, probably due to perceived lack of suitable XC functionals that would conform with ensemble densities. The latter hurdle can be circumvented by employing for the individual energies, E_0 and E_1, the same ensemble representation as was used in Eqs. (4) and (6), and in the REKS method in general.

SA-REKS Method

Let us consider a model system with two strongly correlated electrons, such as the H_2 molecule at the bondlength stretched beyond the Coulson–Fischer point. Restricting ourselves to a minimal basis, the ground state wavefunction of such a system can be represented by Eq. (21),

$$\Phi_0 = \sqrt{\frac{n_a}{2}}\left|\phi_a\overline{\phi}_a\right| - \sqrt{\frac{n_b}{2}}\left|\phi_b\overline{\phi}_b\right| \tag{21}$$

where ϕ_a and ϕ_b can be the bonding ($1\sigma_g$) and antibonding ($1\sigma_u$) orbitals of H_2. Excitation of a single electron in the (2,2) active space leads to a singlet excited state Φ_1 that can be represented by the wavefunction in Eq. (22).

$$\Phi_1 = \sqrt{\frac{1}{2}}\left|\phi_a\overline{\phi}_b\right| + \sqrt{\frac{1}{2}}\left|\phi_b\overline{\phi}_a\right| \tag{22}$$

As, for a homosymmetric biradical such as the dissociating H_2, the two states, Φ_0 and Φ_1, belong to

different symmetry species and, hence, do not interact with one another, an ensemble of the two states can be constructed and the orbitals ϕ_a and ϕ_b be obtained from variational optimization of the ensemble energy.[41] In the framework of REKS methodology, the energy of the Φ_0 state can be obtained using the REKS(2,2) method and the energy of the Φ_1 state can be obtained with the use of the ROKS method for an open-shell singlet (OSS) state.[87,88] In the latter approach, the energy of the OSS state Φ_1 is given by Eq. (23).[87,88]

$$E^{\mathrm{ROKS}}\left[\rho_s\right] = E\left[\ldots \phi_a\overline{\phi}_b\right] - \frac{1}{2}E\left[\ldots \phi_a\phi_b\right] + E\left[\ldots \overline{\phi}_a\phi_b\right] - \frac{1}{2}E\left[\ldots \overline{\phi}_a\overline{\phi}_b\right] \quad (23)$$

Thus, this leads to the SA-REKS energy expression (24),

$$E_{\omega}^{\text{SA-REKS}} = (1-\omega)\,E^{\mathrm{REKS(2,2)}} + \omega E^{\mathrm{ROKS}} \quad (24)$$

which is to be minimized with respect to the orbitals and FONs of the active orbitals of the REKS(2,2) energy (8). Typically, equal weighting factors, that is $\omega = 1/2$, are used in practical calculations with the SA-REKS method.[41] Having minimized the energy (24) and obtained the orbitals, the individual energies, $E^{\mathrm{REKS(2,2)}}$ and E^{ROKS}, are calculated using the common set of orbitals and the excitation energy is obtained from Eq. (20). For obtaining the SA-REKS orbitals, the same one-electron equations as were used for the REKS method could be employed, however with modified weighting factors λ_L in Eqs. (12) and (13), which now become Eq. (25).

$$\lambda_1 = (1-\omega)\frac{n_a}{2};\ \lambda_2 = (1-\omega)\frac{n_b}{2};$$
$$\lambda_3 = \lambda_5 = \omega - \frac{1-\omega}{2}f\left(n_a, n_b\right);$$
$$\lambda_4 = \lambda_6 = \frac{1-\omega}{2}f\left(n_a, n_b\right) - \frac{\omega}{2} \quad (25)$$

The analytic energy derivatives for the averaged state can be calculated by Eq. (16) where no orbital-response part is needed as the SA-REKS orbitals satisfy the variational condition (14) for the averaged energy functional. However, for obtaining the energy gradient of the individual states, the REKS and the OSS states, the orbital response part in Eq. (16) has to be calculated. The elements ${}^{a}U_{ji}^{X}$ of the orbital response matrix can be obtained from the coupled-perturbed REKS (CP-REKS) equations derived by differentiation of the variational conditions in Eq. (14).

SI-SA-REKS Method

The defined SA-REKS method is capable of describing the ground and one of the singlet excited states of a homosymmetric biradical. If one deals with a heterosymmetric system, such as, e.g., dissociating LiH molecule, the two states defined in the minimal basis set in Eqs (21) and (22) will no longer be decoupled from one another.[42,43] To decouple them and to construct an ensemble as in Eq. (18) one can obtain new states from $E^{\mathrm{REKS(2,2)}}$ and E^{ROKS} by solving a 2×2 secular problem with the Hamiltonian matrix spanning the two energies as the diagonal elements and the off-diagonal element given in Eq. (26),

$$H_{01} = \sqrt{n_a}\langle\phi_b|n_a\hat{F}_a|\phi_a\rangle - \sqrt{n_b}\langle\phi_a|n_b\hat{F}_b|\phi_b\rangle = \left(\sqrt{n_a} - \sqrt{n_b}\right)\varepsilon_{ab} \quad (26)$$

which was obtained by the application of Slater-Condon rules to a 2×2 problem in the space of the two configuration state functions (CSFs) Φ_0 and Φ_1 and the variational condition for the orbitals, Eq. (14).[42,43] In Eq. (26), ε_{ab} is the Lagrange multiplier between the active orbitals, ϕ_a and ϕ_b, see Eq. (11). As the two states, Φ_0 and Φ_1, are mutually orthogonal, a sum of the new energies E_0 and E_1 obtained from the above secular problem remains invariant and the orbitals can still be obtained from the SA-REKS one-electron equations, provided that $\omega = 1/2$ was used in Eq. (24). This modification of the SA-REKS formalism was dubbed SI-SA-REKS method and it was found that the use of the state-interaction procedure is important for obtaining the correct shape of the ground and excited state PESs in the vicinity of conical intersections.[42,43] For other situations, when the energy gap between the S_0 and S_1 states is sufficiently large, the SI-SA-REKS method yields almost the same excitation energies as the SA-REKS ones.[49]

The SA-REKS and SI-SA-REKS methods described above operate with only two many-electron states, the ground and one of the excited states. In principle, it is possible to extend this formalism to multiple excited states; however, one would need to derive proper energy expressions for the extra excited states. Perhaps, the simplest procedure to extend SI-SA-REKS beyond two states is to include a state obtained by double excitation of the Φ_0 state (21), which is given in Eq. (27).[49]

$$\Phi_2 = \sqrt{\frac{n_b}{2}}\left|\phi_a\overline{\phi}_a\right| + \sqrt{\frac{n_a}{2}}\left|\phi_b\overline{\phi}_b\right| \quad (27)$$

Usually, this is a high lying state with the energy $E_2^{\mathrm{REKS(2,2)}}$ that can be obtained using Eq. (8) in which the sign of the coefficients λ_k, $k \in [3,6]$ (see Eq. (13)) is

inverted and the coefficients λ_1 and λ_2 are swapped.[49] The inclusion of this state may however become important in the situations when the $E_{a\bar{a}} - E_{b\bar{b}}$ energy difference becomes very small, e.g., during electron transfer caused by the application of external stimuli (electric field, geometric distortion).[49] The effect of this state on the SI-SA-REKS energies can be taken into account via a secular problem in the space of three states, Φ_0, Φ_1, and Φ_2, and the matrix that spans the $E^{\mathrm{REKS(2,2)}}$, E^{ROKS}, and $E_2^{\mathrm{REKS(2,2)}}$ energies as the diagonal elements and the off-diagonal elements defined in Eq. (26) and in Eq. (28) that was obtained similarly to (26).[49]

$$H_{12} = \left(\sqrt{n_a} + \sqrt{n_b}\right)\epsilon_{ab}\ ;\ H_{02} = 0 \qquad (28)$$

In the following, a number of examples that illustrate the use and performance of the described SA-REKS and SI-SA-REKS methods will be given. Similar to the section about applications of the REKS method, the emphasis will be on qualitative aspects of the problems that can be solved by the use of these approaches rather than on collecting MAD (mean absolute deviation) numbers characterizing the quantitative aspects.

Applications of the SA-REKS and SI-SA-REKS Methods

Perhaps the simplest situation where the use of the SA-REKS (or SI-SA-REKS) method becomes necessary is the description of the ground and lowest singlet excited state of a system with dissociating bond.[41,89] Let us take the H_2 molecule as an example and inspect its ground $^1\Sigma_g^+$ and its lowest excited $^1\Sigma_u^+$ states. Near the equilibrium distance, the ground state is represented by a single KS determinant $\left|\sigma_g\overline{\sigma}_g\right|$ and the excited state is a state of the OSS type $\frac{1}{\sqrt{2}}\left|\sigma_g\overline{\sigma}_u\right| - \frac{1}{\sqrt{2}}\left|\overline{\sigma}_g\sigma_u\right|$. When the H–H bond is stretched beyond the Coulson–Fischer point, the ground state becomes a MR state of the type given in Eq. (21), whereas the excited state still remains the OSS type. As was discussed earlier, the description of the ground state breaks down at the single-reference RKS level and the correct dissociation curve of the H_2 molecule cannot be recovered (see Figure 2). As a consequence, the traditional linear-response TD-DFT based on the single KS reference state fails to describe correctly the dependence of the $^1\Sigma_u^+ \leftarrow {}^1\Sigma_g^+$ excitation energy of the H–H distance and, for long interatomic separations, the TD-DFT excitation energy vanishes.[89]

The SA-REKS method (SI-SA-REKS and SA-REKS are identical for a homosymmetric system), due to the correct inclusion of the MR description for the ground state, is capable of recovering the correct distance dependence of the ground and excited state potential energy curves and, consequently, of the excitation energy.[41] This is illustrated in Figure 7 where the results of the TD-DFT and SA-REKS calculations carried out with the use of the CAM-B3LYP density functional and the cc-pV5Z basis set[24] are compared with the exact excitation energy curve from Ref 59. Although the SA-REKS excitation energy curve is shifted down as compared with the exact curve (this feature is XC functional dependent and other functionals yield smaller discrepancy),[41] it has a shallow minimum at R_{HH} ca 4.3 bohr, which is similar to the exact curve that minimizes at 4.1 bohr. The H–H bond dissociation is correctly described at the SA-REKS level: The ground state at long distances has a purely covalent diradical character and flattens out at the energy level of two neutral H atoms. The excited state has a purely ionic character and corresponds to two resonating valence configurations, H^+–H^- and H^-–H^+. These results demonstrate that the SA-REKS method is capable of correctly describing the ground and excited states of dissociating homopolar chemical bond.

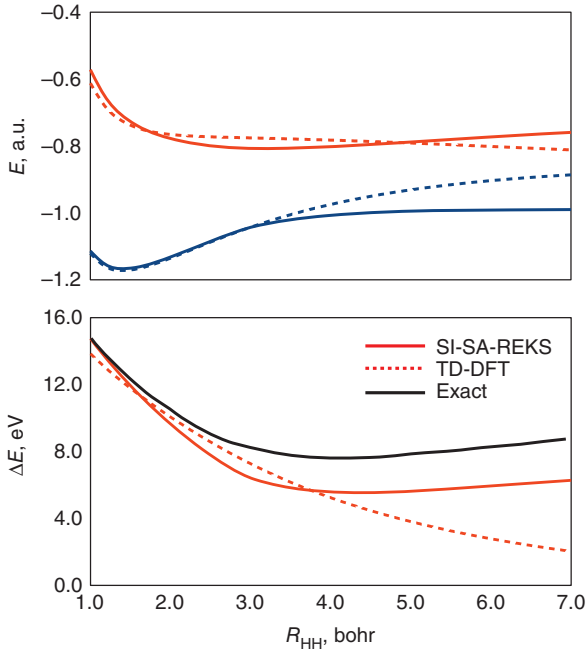

FIGURE 7 | Potential energy curves (upper panel) of the $^1\Sigma_g^+$ and $^1\Sigma_u^+$ states of H_2 and the $^1\Sigma_u^+ \leftarrow {}^1\Sigma_g^+$ excitation energy (lower panel) as a function of the H–H distance. Solid colored curves (blue for the ground state and red for the excited state) represent the results of the SA-REKS calculations, dashed colored curves refer to TD-DFT, and black curve is the exact excitation energy obtained from the results of Ref 59. DFT calculations employ the CAM-B3LYP density functional and the cc-pV5Z basis set modified as in Ref 24.

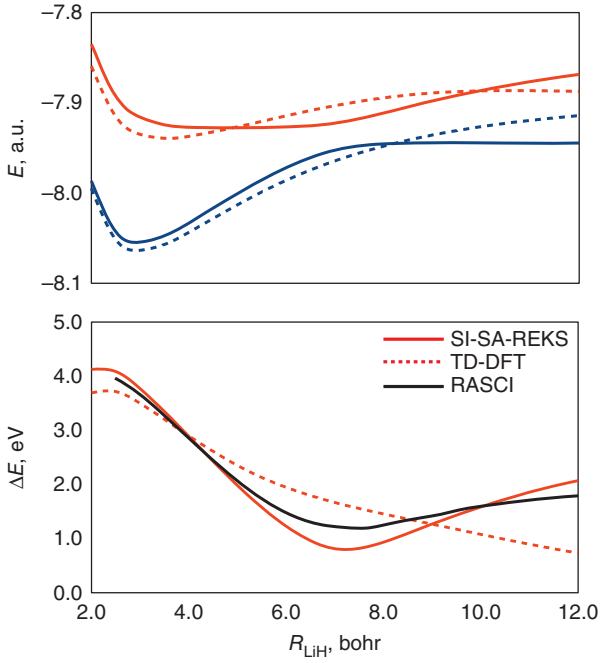

FIGURE 8 | Potential energy curves (upper panel) of the $x^1\Sigma^+$ and $a^1\Sigma^+$ states of LiH and the $x^1\Sigma^+ \leftarrow a^1\Sigma^+$ excitation energy (lower panel) as a function of the Li-H distance. Solid curves—SI-SA-REKS results, dashed curves—TD-DFT results. DFT calculations employ the CAM-B3LYP functional and aug-cc-pVTZ basis set. The reference RASCI excitation energy curve (solid black) is taken from Ref 90.

Turning to dissociation of a heteropolar chemical bond, let us briefly review the ground and excited states of dissociating LiH molecule. The $x^1\Sigma^+ \leftarrow a^1\Sigma^+$ excitation energy dependence on the Li–H interatomic distance has been recently studied[90] using the restricted active space CI (RASCI) method with aug-cc-pVTZ basis set. Figure 8 shows the potential energy curves and the excitation energy curve of LiH obtained from the SI-SA-REKS and TD-DFT calculations. As is apparent from Figure 8 (see also the discussion around Figure 3), the ground and excited states of LiH undergo an avoided crossing near ca 7.0 bohr and the ground state changes its character from ionic to covalent. This is correctly described by the SI-SA-REKS approach which yields the correct profile of the ground and excited state potential energy curves in a semi-quantitative agreement with the reference ab initio calculations. The TD-DFT method fails to take into account the change of the character of the ground state (this is inherited from the RKS calculation) and, consequently, fails to produce the correct description of the excited state of LiH. The TD-DFT excitation energy goes gradually to zero with the increasing Li–H distance and does not show any signature of an avoided crossing between the ionic and covalent states.

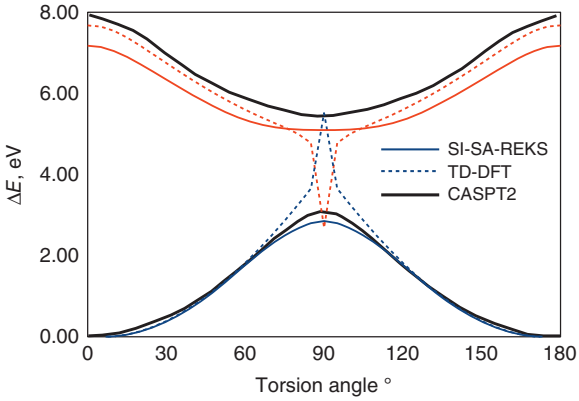

FIGURE 9 | Profile of the potential energy surfaces of the ground $^1A_1$ and excited $^1B_1$ states (under the D_2 symmetry) along the double bond torsion mode of C_2H_4. Black lines—CASPT2/6-31G* results from Ref 41 solid colored lines—SI-SA-REKS results, and dashed colored lines—TD-DFT results. DFT calculations employ the CAM-B3LYP density functional and 6-31G* basis set.

The above two examples, H_2 and LiH, demonstrate that the SI-SA-REKS method is capable of describing the bond dissociation proper way. Although these were only small diatomic molecules, the same observation holds true for polyatomic molecules.[41] To illustrate this statement, Figure 9 shows profiles of the ground $^1A_1$ and excited $^1B_1$ PESs of ethylene along the double bond torsion mode. In Ref 41 this system has been studied using the SA-REKS methodology where it was compared with the results of the CASPT2 calculations. The CASPT2 curves are reproduced in Figure 9 and compared with the SA-SA-REKS and TD-DFT curves obtained using the CAM-B3LYP functional (not used in Ref 41). This comparison demonstrates that the REKS methodology correctly describes the ground and excited state PESs along the torsion mode, while TD-DFT fails to produce correct results near ca 90° of torsion, where the ground state of C_2H_4 becomes strongly correlated.

The SI-SA-REKS method has been also benchmarked[48] for valence excitations in ordinary (that is not strongly correlated) organic molecules and was found to be as accurate as the linear response methods, such as TD-DFT and ADC(2)[91–94] (second-order algebraic diagrammatic construction; a method based on second-order polarization propagator approach). For instance, when using the aug-cc-pVTZ basis set to describe valence $\pi \rightarrow \pi^*$ and $n \rightarrow \pi^*$ excitations in a set of 15 aliphatic and aromatic hydrocarbons, the MAD of the calculated excitation energies from the best estimates[95] was 0.43 eV for SI-SA-RE-BH&HLYP, 0.47 eV for TD-BH&HLYP, and 0.43 eV for ADC(2).[48] Generally, for valence electronic transitions, the accuracy of the SI-SA-REKS excitation energies is defined by the density functional

TABLE 2 | Excitation Energies (eV) of the Lowest CT Transitions of the Ar-TCNE Adducts[49]

	BLYP		B3LYP		CAM-B3LYP			
Arene	TD-DFT	SI-SA-REKS	TD-DFT	SI-SA-REKS	TD-DFT	SI-SA-REKS	Lit.[1]	Exp.[2]
Benzene	1.54	3.53	2.06	3.70	3.03	3.68	3.8	3.59
Naphthalene	0.34	2.28	0.90	2.54	1.96	2.61	2.7	2.60
Toluene	1.37	2.72	1.81	3.11	2.72	3.46	3.4	3.36
o-Xylene	1.47	2.61	1.54	2.95	2.46	3.15	3.0	3.15
MAD[3]	2.00	0.39	1.60	0.16	0.63	0.05	0.13	

[1]Literature data: results of TD-DFT calculations using the tuned range-separated BNL functional from Ref 100.
[2]Gas phase excitation energies of CT transitions from Ref 101.
[3]Mean absolute deviation from the experimental data.

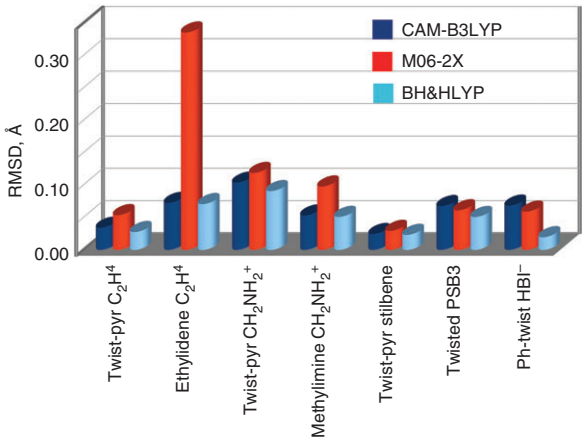

FIGURE 10 | RMSD (Å) of the geometries at the minimum energy CI points of a number of organic molecules optimized using the SI-SA-REKS method from the target geometries obtained using *ab initio* multi-reference methods, CASPT2 and MRSDCI. (Reprinted with permission (ACS AuthorChoice) from Ref 43. Copyright 2013 American Chemical Society)

employed, much in the same way as it occurs for TD-DFT.[48]

Obviously, the ability of SI-SA-REKS method to describe electronic transitions in strongly correlated molecules enables one to apply this method beyond the realm of applicability of the conventional linear-response TD-DFT. Thus the SI-SA-REKS method has been successfully used to study conical intersections (CIs, intersections between PESs of the electronic states with the same spin and space symmetry) between the ground and the lowest singlet excited states in a series of organic molecules, biological chromophores, and synthetic molecular machines.[42,43,96,97] The geometries of molecules at the minimum energy CIs optimized using SI-SA-REKS in connection with several density functionals deviate from the reference geometries obtained using the high-level ab initio MR methods, CASPT2 and MRSDCI, by less than 0.1 Å on average.[43] This is illustrated in Figure 10 where, for a few organic molecules, the root mean square deviations (RMSDs) of the SI-SA-REKS geometries at the minimum energy CI points from the MR *ab initio* geometries are shown.[43] The SI-SA-REKS method is also capable of accurately computing the non-adiabatic coupling parameters between the ground and excited states in the form of the branching plane vectors[98] of conical intersections.[99] The branching plane vectors are obtained by differentiation of the respective parts of the SI-SA-REKS energy expression, see Refs 96, 97, and 99 for the detailed expressions.

Besides the described strongly correlated and ordinary systems, the SI-SA-REKS method has been applied to study the charge transfer excitations in organic donor–acceptor systems.[49] Although it was not originally designed to specifically target this type of excitations, the accurate description of which is notoriously difficult for the linear-response methods,[84,85] the SI-SA-REKS method was found to be surprisingly accurate even when used in connection with the usual GGA density functionals. Table 2 reports excitation energies of the lowest CT transitions in a series of arene-TCNE (tetracyanoethylene) complexes, for which gas phase absorption energies are available.[101] For these excitations, TD-DFT results deviate by a wide margin from the experimental figures even when a range-separated XC functional (CAM-B3LYP) is used. Only fine tuning of the parameters of a range-separated XC functional (these functionals were specifically designed to treat the CT excitations) brings the MAD to an acceptable level.[100] The accuracy of the fine tuned range-separated functional is easily surpassed by the SI-SA-REKS method employed in connection with the stock parameterization of a hybrid (B3LYP or BH&HLYP) or a range-separated (CAM-B3LYP) functional.[49] The observed excellent performance of SI-SA-REKS, which implements the ΔSCF approach to obtaining excitation energies, is consistent with the analysis of the description of various types of excitations undertaken by Ziegler et al.[84,85] who showed that it is the linear response approximation

and not the density functional that is to blame for a ludicrous performance of TD-DFT. Although SI-SA-REKS can be used in connection with the fine tuned range-separated functionals,[100] no such tuning is necessary as evidenced by the results in Table 2.

To round up this section, ensemble DFT for excited states as implemented in the SI-SA-REKS method is a versatile and accurate approach to the calculation of various types of excitations in molecular systems. A wide range of excited states, which are otherwise not accessible with the use of TD-DFT, can be studied, including the CT excitations,[49] excitations in extended π-conjugated systems, such as cyanines and polyacenes,[48] excitations in molecules undergoing bond breaking/bond formation,[41] conical intersections between the ground and excited electronic states,[42,43,97,99] etc. It is also noteworthy that the SI-SA-REKS results can be obtained at an essentially mean-field cost, avoiding a steeper scaling of the linear response formalism of TD-DFT.

CONCLUSIONS AND OUTLOOK

Ensemble DFT is an active field of research that holds promise to considerably improve the level of theoretical description of the ground and excited states of strongly correlated molecular systems. Although there is an ongoing effort to further develop the theoretical background of ensemble DFT, this theory still did not find its way to the wide practical use by computational chemists. Perhaps, the perceived lack of practical implementations of ensemble DFT holds down its adoption by a wider computational chemistry community. It was thus the purpose of this review to introduce the theoretical background and practical capabilities of a method that implements ensemble DFT, the REKS method.

REKS method makes ensemble DFT feasible; it has been already successfully applied to study various types of strongly correlated molecular systems, including biradicals, anti-ferromagnetically coupled molecules and molecular crystals, excited states and conical intersections, to name just a few. An important advantage of the REKS method is that it makes computational study of large molecular systems affordable by providing accurate theoretical description of their electronic structure at a moderate mean-field computational cost.

The current implementation of the method is not without certain limitations. The size of the active space (the number of strongly correlated electrons) is currently limited to two electrons in two fractionally occupied orbitals. This limitation is to be lifted in the near future; there has been already work on the method extension and this work will be continued. The number of excited states accessible through the state-averaged REKS formalism needs to be increased to afford computation of complete molecular electronic spectra. Such an extension of the method can be achieved by merging it with the response approach to the calculation of excitation energies[84,85] and deriving a time-dependent extension of the REKS method. This task is closely related with the implementation of the analytic energy derivatives (first and higher order) of the SA-REKS and SI-SA-REKS methods which will considerably improve the prospects of practical applicability of the methods. Taken together, the foreseen developments will bring the REKS methodology on an equal footing with the currently used methods of computational chemistry and will enable one to routinely study molecular systems of realistic (i.e., large and very large) size without a frightening perspective that the wall-clock time may exceed the life expectancy.

NOTE

[a] Equation (6) is proved in Theorem 4.2 of Ref 25 for the ensemble density (4) (or, equivalently, (5)) and Theorem 4.3 of Ref 25 proves the equivalence of the ensemble energy functional in Eq. (6) and the Hohenberg-Kohn functional for PS-VR densities. The fact that any positive definite physical density is fermion E-VR is proved in Theorem 5.1 of Refs 26 and 27 and Theorem 6.1 of Refs 26 and 27 proves the differentiability of the energy functional (6) on the set of E-VR densities.

REFERENCES

1. Löwdin P-O. Quantum theory of many-particle systems. I. Physical interpretations by means of density matrices, natural spin-orbitals, and convergence problems in the method of configurational interaction. *Phys Rev* 1955, 97:1474–1489.
2. Löwdin P-O. Quantum theory of many-particle systems. III. Extension of the Hartree-Fock scheme to include degenerate systems and correlation effects. *Phys Rev* 1955, 97:1509–1520.
3. Sinanoglŭ O. Many-electron theory of atoms, molecules and their interactions. *Adv Chem Phys* 1964, 6:315–412.
4. Andersson K, Roos BO. In: Yarkony DR, ed. *Modern Electronic Structure Theory, Advanced Series in*

Physical Chemsitry, vol. 2 Part I. Singapore: World Scientific; 1995, 55.

5. Andersson K, Malmqvist P-Å, Roos BO. Second-order perturbation theory with a complete active space self-consistent field reference function. *J Chem Phys* 1992, 96:1218–1226.
6. Evangelista FA, Allen WD, Schaefer HF. High-order excitations in state-universal and state-specific multireference coupled cluster theories: Model systems. *J Chem Phys* 2006, 125:154113.
7. Evangelista FA, Allen WD, Schaefer HF. Coupling term derivation and general implementation of state-specific multireference coupled cluster theories. *J Chem Phys* 2007, 127:024102.
8. Kohn W, Sham LJ. Self-consistent equations including exchange and correlation effects. *Phys Rev* 1965, 140: A1133–A1138.
9. Hohenberg P, Kohn W. Inhomogeneous electron gas. *Phys Rev* 1964, 136:B864–B871.
10. Cohen AJ, Handy NC. Dynamic correlation. *Mol Phys* 2001, 99:607–615.
11. Cremer D. Density functional theory: coverage of dynamic and non-dynamic electron correlation effects. *Mol Phys* 2001, 99:1899–1940.
12. Wang SG, Schwarz WHE. Simulation of nondynamical correlation in density functional calculations by the optimized fractional orbital occupation approach: application to the potential energy surfaces of O_3 and SO_2. *J Chem Phys* 1996, 105:4641–4648.
13. Noodleman L. Valence bond description of antiferromagnetic coupling in transition metal dimers. *J Chem Phys* 1981, 74:5737–5743.
14. Noodleman L, Davidson ER. Ligand spin polarization and antiferromagnetic coupling in transition metal dimers. *Chem Phys* 1986, 109:131–143.
15. Ciofini I, Illas F, Adamo C. Performance of the τ-dependent functionals in predicting the magnetic coupling of ionic antiferromagnetic insulators. *J Chem Phys* 2004, 120:3811–3816.
16. Adamo C, Barone V, Bencini A, Broer R, Filatov M, Harrison NM, Illas F, Malrieu JP, Moreira I de PR. Comment on "About the calculation of exchange coupling constants using density-functional theory: The role of the self-interaction error" [J. Chem. Phys. 123, 164110, 2005]. *J Chem Phys* 2006, 124:107101.
17. Caballol R, Castell O, Illas F, Malrieu JP, Moreira I de PR. Remarks on the proper use of the broken symmetry approach to magnetic coupling. *J Phys Chem A* 1997, 101:7860–7866.
18. Moreira I de PR, Illas F. A unified view of the theoretical description of magnetic coupling in molecular chemistry and solid state physics. *Phys Chem Chem Phys* 2006, 8:1645–1659.
19. Pollet R, Savin A, Leininger T, Stoll H. Combining multideterminantal wave functions with density functionals to handle near-degeneracy in atoms and molecules. *J Chem Phys* 2002, 116:1250–1258.
20. McDouall JJW. Combining two-body density functionals with multiconfigurational wavefunctions: diatomic molecules. *Mol Phys* 2003, 101:361–371.
21. Gräfenstein J, Cremer D. Development of a CAS-DFT method covering non-dynamical and dynamical electron correlation in a balanced way. *Mol Phys* 2005, 103:279–308.
22. Cremer D, Filatov M, Polo V, Kraka E, Shaik S. Implicit and explicit coverage of multi-reference effects by density functional theory. *Int J Mol Sci* 2002, 3:604–638.
23. Burke K, Perdew JP, Ernzerhof M. Why semilocal functionals work: accuracy of the on-top pair density and importance of system averaging. *J Chem Phys* 1998, 109:3760–3771.
24. Schipper PRT, Gritsenko OV, Baerends EJ. Benchmark calculations of chemical reactions in density functional theory: Comparison of the accurate Kohn–Sham solution with generalized gradient approximations for the H_2+H and H_2+H_2 reactions J. *Chem Phys* 1999, 111: 4056–4067.
25. Lieb EH. Density Functionals for Coulomb Systems. *Int J Quantum Chem* 1983, 24:243–277.
26. Englisch H, Englisch R. Exact density functionals for ground-state energies. I. General results. *Phys Stat Sol b* 1984, 123:711–721.
27. Englisch H, Englisch R. Exact density functionals for ground-state energies II. Details and remarks. *Phys Stat Sol b* 1984, 124:373–379.
28. Ullrich CA, Kohn W. Kohn-Sham theory for ground-state ensembles. *Phys Rev Lett* 2001, 87: 093001.
29. Schipper PRT, Gritsenko OV, Baerends EJ. One-determinantal pure state versus ensemble Kohn-Sham solutions in the case of strong electron correlation: CH_2 and C_2. *Theor Chem Acc* 1998, 99:329–343.
30. Morrison RC. Electron correlation and noninteracting v-representability in density functional theory: the Be isoelectronic series. *J Chem Phys* 2002, 117: 10506–10511.
31. Slater J, Mann JB, Wilson TM, Wood JH. Nonintegral occupation numbers in transition atoms in crystals. *Phys Rev* 1969, 184:672–694.
32. Dunlap BI. Symmetry and degeneracy in Xα and density functional theory. *Adv Chem Phys* 1987, 69: 287–318.
33. Filatov M, Shaik S. A spin-restricted ensemble-referenced Kohn-Sham method and its application to diradicaloid situations. *Chem Phys Lett* 1999, 304: 429–437.
34. Filatov M, Shaik S. Diradicaloids: description by the spin-restricted, ensemble-referenced Kohn-Sham density functional method. *J Phys Chem A* 2000, 104:6628–6636.

35. Filatov M, Shaik S. Tetramethyleneethane (TME) diradical: experiment and density functional theory reach an agreement. *J Phys Chem A* 1999, 103: 8885–8889.
36. Illas F, Moreira I de PR, Bofill JM, Filatov M. Extent and limitations of density-functional theory in describing magnetic systems. *Phys Rev B* 2004, 70: 132414.
37. Illas F, Moreira I de PR, Bofill JM, Filatov M. Spin symmetry requirements in density functional theory: the proper way to predict magnetic coupling constants in molecules and solids. *Theory Chem Acc* 2006, 116:587–597.
38. Moreira I de PR, Costa R, Filatov M, Illas F. Restricted ensemble-referenced Kohn-Sham versus broken symmetry approaches in density functional theory: magnetic coupling in Cu binuclear complexes. *J Chem Theory Comput* 2007, 3:764–774.
39. Filatov M. On multiferroicity of TTF-CA molecular crystal. *Phys Chem Chem Phys* 2011, 13:144–148.
40. Filatov M. Antiferromagnetic interactions in the quarter-filled organic conductor $(EDO\text{-}TTF)_2PF_6$. *Phys Chem Chem Phys* 2011, 13:12328–12334.
41. Kazaryan A, Heuver J, Filatov M. Excitation energies from spin-restricted ensemble-referenced Kohn-Sham method: a state-averaged approach. *J Phys Chem A* 2008, 112:12980–12988.
42. Huix-Rotllant M, Filatov M, Gozem S, Schapiro I, Olivucci M, Ferré N. Assessment of density functional theory for describing the correlation effects on the ground and excited state potential energy surfaces of a retinal chromophore model. *J Chem Theory Comput* 2013, 9:3917–3932.
43. Filatov M. Assessment of density functional methods for obtaining geometries at conical intersections in organic molecules. *J Chem Theory Comput* 2013, 9: 4526–4541.
44. Kazaryan A, Filatov M. Density functional study of the ground and excited state potential energy surfaces of a light-driven rotary molecular motor (3R,3'R)-(P,P)-trans-1,1',2,2',3,3',4,4'-octahydro-3,3'-dimethyl-4,4'-biphenanthrylidene. *J Phys Chem A* 2009, 113:11630–11634.
45. Kazaryan A, Lan Z, Schäfer LV, Thiel W, Filatov M. Surface hopping excited-state dynamics study of the photoisomerization of a light-driven fluorene molecular rotary motor. *J Chem Theory Comput* 2011, 7:2189–2199.
46. Filatov M. Theoretical study of the photochemistry of a reversible three-state Bis-thiaxanthylidene molecular switch. *ChemPhysChem* 2011, 12:3348–3353.
47. Kazaryan A, Kistemaker JCM, Schäfer LV, Browne WR, Feringa BL, Filatov M. Understanding the dynamics behind the photoisomerization of a light-driven fluorene molecular rotary motor. *J Phys Chem A* 2010, 114:5058–5067.
48. Filatov M, Huix-Rotllant M. Assessment of density functional theory based ΔSCF (self-consistent field) and linear response methods for longest wavelength excited states of extended π-conjugated molecular systems. *J Chem Phys* 2014, 141:024112.
49. Filatov M. Description of electron transfer in the ground and excited states of organic donor-acceptor systems by single-reference and multi-reference density functional methods. *J Chem Phys* 2014, 141:124123.
50. Noziéres P, Pines D. *The Theory of Quantum Liquids*. Cambridge, MA: Perseus Books Publishing LLC; 1966, 296–298.
51. Becke AD. Correlation energy of an inhomogeneous electron gas: a coordinate-space model. *J Chem Phys* 1988, 88:1053–1062.
52. Zhao Q, Morrison RC, Parr RG. From electron densities to Kohn-Sham kinetic energies, orbital energies, exchange-correlation potentials, and exchange-correlation energies. *Phys Rev A* 1994, 50:2138–2142.
53. Franck O, Fromager E. Generalised adiabatic connection in ensemble density-functional theory for excited states: example of the H_2 molecule. *Mol Phys* 2014, 112:1684–1701.
54. Giesbertz KJH, Baerends EJ. Aufbau derived from a unified treatment of occupation numbers in Hartree–Fock, Kohn–Sham, and natural orbital theories with the Karush–Kuhn–Tucker conditions for the inequality constraints $n_i \leq 1$ and $n_i \geq 0$. *J Chem Phys* 2010, 132:194108.
55. Fernandez JJ, Kollmar C, Filatov M. Obtaining stable solutions of the optimized-effective-potential method in the basis set representation. *Phys Rev A* 2010, 82:022508.
56. Hirao K, Nakatsuji H. General SCF operator satisfying correct variational condition. *J Chem Phys* 1973, 59: 1457–1462.
57. Roothaan CCJ. Self-consistent field theory for open shells of electronic systems. *Rev Mod Phys* 1960, 32: 179–185.
58. Goddard WA, Dunning TH, Hunt WJ, Hay PJ. Generalized valence bond description of bonding in low-lying states of molecules. *Acc Chem Res* 1973, 6: 368–376.
59. Kołos W, Wolniewicz L. Potential-energy curves for the $X^1\Sigma_g^+$, $b^3\Sigma_u^+$, and C $^1\Pi_u$ states of the hydrogen molecule. *J Chem Phys* 1965, 43:2429–2441.
60. Coulson CA, Fischer I. Notes on the molecular orbital treatment of the hydrogen molecule. *Philos Mag* 1949, 40:386–393.
61. Yanai T, Tew D, Handy NC. A new hybrid exchange-correlation functional using the Coulomb-attenuating method (CAM-B3LYP). *Chem Phys Lett* 2004, 393: 51–57.
62. Takeda R, Yamanaka S, Yamaguchi K. Resonating broken-symmetry approach to biradicals and polyradicals. *Int J Quant Chem* 2006, 106:3303–3311.

63. Goel S, Masunov AE. Pairwise spin-contamination correction method and DFT study of MnH and H_2 dissociation curves. In: Allen G, Nabrzyski J, Seidel E, van Albada G, Dongarra J, Sloot PMA, eds. *Computational Science – ICCS 2009*. Lecture Notes in Computer Science, vol. 5545. Berlin, Heidelberg: Springer; 2009, 141–150.
64. Furche F. Molecular tests of the random phase approximation to the exchange-correlation energy functional. *Phys Rev B* 2001, 64:195120.
65. Olsen T, Thygesen KS. Static correlation beyond the random phase approximation: dissociating H_2 with the Bethe-Salpeter equation and time-dependent GW. *J Chem Phys* 2014, 140:164116.
66. Stwalley WC, Zemke WT. Spectroscopy and structure of the lithium hydride molecules and ions. *J Phys Chem Ref Data* 1993, 22:87–112.
67. Huber KP, Herzberg G. *Molecular Spectra and Molecular Structure. IV. Constants of Diatomic Molecules*. New York: Van Nostrand Reinhold Co.; 1979.
68. Woodward RB, Hoffmann R. The conservation of orbital symmetry. *Angew Chem Int Ed Engl* 1969, 8:781–853.
69. Hoffmann R, Woodward RB. Selection rules for concerted cycloaddition reactions. *J Am Chem Soc* 1965, 87:2046–2048.
70. Hoffmann R, Woodward RB. Stereochemistry of electrocyclic reactions. *J Am Chem Soc* 1965, 87: 395–397.
71. Filatov M, Shaik S, Woeller M, Grimme S, Peyerimhoff SD. Locked alkenes with a short triplet state lifetime. *Chem Phys Lett* 2000, 316:135–140.
72. Salem L, Rowland C. The electronic properties of diradicals. *Angew Chem Int Ed* 1972, 11:92–111.
73. Li X, Paldus J. Electronic structure of organic diradicals: evaluation of the performance of coupled-cluster methods. *J Chem Phys* 2008, 129:174101.
74. Kraka E, Cremer D. Ortho-, meta-, and para-benzyne. A comparative CCSD (T) investigation. *Chem Phys Lett* 1993, 216:333–340.
75. Wenthold PG, Squires RR, Lineberger WC. Ultraviolet photoelectron spectroscopy of the o-, m-, and p-benzyne negative ions. Electron affinities and singlet-triplet splittings for o-, m-, and p-benzyne. *J Am Chem Soc* 1998, 120:5279–5290.
76. Dowd P. Tetramethyleneethane. *J Am Chem Soc* 1970, 92:1066–1068.
77. Borden WT, Lineberger WC. The synergy between qualitative theory, quantitative calculations, and direct experiments in understanding, calculating, and measuring the energy differences between the lowest singlet and triplet states of organic diradicals. *Phys Chem Chem Phys* 2011, 13:11792–11813.
78. Clifford EP, Wenthold PG, Lineberger WC, Ellison GB, Wang CX, Grabowski JJ, Vila F, Jordan KD. Properties of tetramethyleneethane (TME) as revealed by ion chemistry and ion photoelectron spectroscopy. *J Chem Soc Perkin Trans* 1998, 2:1015–1022.
79. Grimme S. Semiempirical GGA-type density functional constructed with a long-range dispersion correction. *J Comput Chem* 2006, 27:1787–1799.
80. Vydrov OA, Van Voorhis T. Nonlocal van der Waals density functional: the simpler the better. *J Chem Phys* 2010, 133:244103.
81. Marques MAL, Gross EKU. Time-dependent density functional theory. In: Fiolhais C, Nogueira F, Marques MAL, eds. *A Primer in Density-Functional Theory*. Lecture Notes in Physics, vol. 620. Berlin: Springer; 2003, 144–184.
82. Casida ME, Huix-Rotllant M. Progress in time-dependent density-functional theory. *Annu Rev Phys Chem* 2012, 63:287–323.
83. Huix-Rotllant M, Ipatov A, Rubio A, Casida ME. Assessment of dressed time-dependent density-functional theory for the low-lying valence states of 28 organic chromophores. *Chem Phys* 2011, 391: 120–129.
84. Krykunov M, Seth M, Ziegler T. Introducing constricted variational density functional theory in its relaxed self-consistent formulation (RSCF-CV-DFT) as an alternative to adiabatic time dependent density functional theory for studies of charge transfer transitions. *J Chem Phys* 2014, 140:18A502.
85. Zhekova H, Krykunov M, Autschbach J, Ziegler T. Applications of time dependent and time independent density functional theory to the first π to π^* transition in cyanine dyes. *J Chem Theory Comput* 2014, 10:3299–3307. doi: 10.1021/ct500292c.
86. Gross EKU, Oliveira LN, Kohn W. Density-functional theory for ensembles of fractionally occupied states. I. Basic formalism. *Phys Rev A* 1988, 37: 2809–2820.
87. Ziegler T, Rauk A, Baerends EJ. On the calculation of multiplet energies by the hartree-fock-slater method. *Theor Chim Acta* 1977, 43:261–271.
88. Filatov M, Shaik S. Spin-restricted density functional approach to the open-shell problem. *Chem Phys Lett* 1998, 288:689–697.
89. Aryasetiawan F, Gunnarsson O, Rubio A. Excitation energies from time-dependent density-functional formalism for small systems. *Europhys Lett* 2002, 57:683–689.
90. Van Meer R, Gritsenko OV, Baerends EJ. Excitation energies with linear response density matrix functional theory along the dissociation coordinate of an electron-pair bond in N-electron systems. *J Chem Phys* 2014, 140:024101.
91. Schirmer J. Beyond the random-phase approximation: a new approximation scheme for the polarization propagator. *Phys Rev A* 1982, 26:2395–2416.

92. Schirmer J, Trofimov AB. An efficient polarization propagator approach to valence electron excitation spectra. *J Phys B At Mol Opt Phys* 1995, 28: 2299–2325.

93. Trofimov AB, Stelter G, Schirmer J. A consistent third-order propagator method for electronic excitation. *J Chem Phys* 1999, 111:9982–9999.

94. Schirmer J, Trofimov AB. Intermediate state representation approach to physical properties of electronically excited molecules. *J Chem Phys* 2004, 120:11449–11464.

95. Silva-Junior MR, Schreiber M, Sauer SPA, Thiel W. Benchmarks for electronically excited states: time-dependent density functional theory and density functional theory based multireference configuration interaction. *J Chem Phys* 2008, 129: 104103.

96. Gozem S, Melaccio F, Valentini A, Filatov M, Huix-Rotllant M, Ferré N, Frutos LM, Angeli C, Krylov AI, Granovsky AA, et al. On the shape of multireference, EOM-CC, and DFT potential energy surfaces at a conical intersection. *J Chem Theory Comput* 2014, 10:3074–3084. doi: 10.1021/ct500154k.

97. Filatov M, Olivucci M. Designing conical intersections for light-driven single molecule rotary motors: from precessional to axial motion. *J Org Chem* 2014, 79:3587–3600.

98. Atchity GJ, Xantheas SS, Ruedenberg K. Potential energy surfaces near intersections. *J Chem Phys* 1991, 95:1862–1876.

99. Nikiforov A, Gamez JA, Thiel W, Huix-Rotllant M, Filatov M. Assessment of approximate computational methods for conical intersections and branching plane vectors in organic molecules. *J Chem Phys* 2014, 141:124122.

100. Stein T, Kronik L, Baer R. Reliable prediction of charge transfer excitations in molecular complexes using time-dependent density functional theory. *J Am Chem Soc* 2009, 131:2818–2820.

101. Hanazaki I. Vapor-phase electron donor-acceptor complexes of tetracyanoethylene and of sulfur dioxide. *J Phys Chem* 1972, 76:1982–1989.